

GROUND SUPPORT FOR CONSTRUCTABILITY OF DEEP UNDERGROUND EXCAVATIONS

Challenge of managing highly stressed ground in civil
and mining projects

Peter K. Kaiser, Professor Emeritus - Bharti School of Engineering,
Laurentian University, Sudbury, Ontario, Canada. pkaiser@laurentian.ca

N° ISBN : 978-2-9701013-8-3

APRIL 2016



ASSOCIATION
INTERNATIONALE DES TUNNELS
ET DE L'ESPACE SOUTERRAIN

AITES

ITA

INTERNATIONAL TUNNELLING
AND UNDERGROUND SPACE
ASSOCIATION

Muirwood lecture 2016 - **GROUND SUPPORT FOR CONSTRUCTABILITY OF DEEP UNDERGROUND EXCAVATIONS**

N°ISBN : 978-2-9701013-8-3 / APRIL 2016 - Layout : Longrine – Avignon – France – www.longrine.fr

The International Tunnelling and Underground Space Association/Association Internationale des Tunnels et de l'Espace Souterrain (ITA/AITES) publishes this report to, in accordance with its statutes, facilitate the exchange of information, in order: to encourage planning of the subsurface for the benefit of the public, environment and sustainable development to promote advances in planning, design, construction, maintenance and safety of tunnels and underground space, by bringing together information thereon and by studying questions related thereto. This report has been prepared by professionals with expertise within the actual subjects. The opinions and statements are based on sources believed to be reliable and in good faith. However, ITA/AITES accepts no responsibility or liability whatsoever with regard to the material published in this report. This material is: information of a general nature only which is not intended to address the specific circumstances of any particular individual or entity; not necessarily comprehensive, complete, accurate or up to date; This material is not professional or legal advice (if you need specific advice, you should always consult a suitably qualified professional).

GROUND SUPPORT FOR CONSTRUCTABILITY OF DEEP UNDERGROUND EXCAVATIONS

Challenge of managing highly stressed ground in civil and mining projects

Peter K. Kaiser, Professor Emeritus - Bharti School of Engineering, Laurentian University, Sudbury, Ontario, Canada pkaiser@laurentian.ca

For the economic and safe construction of deep tunnels, a contractor has to be presented with efficient and effective ground control measures, i.e., support classes that can be rapidly installed and are effective in managing stress-fractured ground. For this purpose, it is necessary to properly anticipate the rock mass behaviour and then provide flexible but reliable means for the support of a shell of stress-damaged ground around the excavation such that a tunnelling project can proceed without unnecessary delays. Stress-driven rock mass failure in brittle rock in the form of gradual ravelling or sudden strainbursting may often slow the tunnelling progress. Both failure processes impose difficult and hazardous conditions for tunnel construction whether the tunnel is advanced by TBM or drilling and blasting.

Robust engineering integrating empirical experience, engineering analysis and sound construction methods provide the key to successful tunnelling and timely project completion. Designs that respect the complexity and variability of the ground, consider the practicality and efficiency of construction, and ensure the effectiveness of ground control measures, lead to fewer project interruptions and, consequently, fewer claims or cost overruns. Robust engineering in highly stressed, brittle failing rock means to design for rock mass degradation and to ensure that all construction tools work well with broken rock.

Some challenges to overcome for economic constructability are engineering design aspects that matter for the selection of the most appropriate excavation technique and the most efficient and effective support systems. This article discusses both fundamental and practical means to better understand and properly document (e.g., in tender documents) the anticipated rock mass and excavation behaviour; better qualify relevant rock mass characteristics and their variability; adopt representative models and inputs to capture the actual rock mass behaviour; and account for practical constraints during construction (i.e., by matching a design to a chosen construction technique). These elements of excavation design are discussed and the impact of naturally variable conditions is reviewed. Guidance is provided for the quantification of anticipated rock mass behaviour near excavations and for the selection of design inputs to arrive at ground control measures that provide both safe and efficient construction. It is discussed how stress-fractured ground is prone to ravelling and how it imposes large deformations due to rock mass bulking. It is concluded that deformation-based support selection principles are most suitable for conditions with stress-fractured ground. Guidance is also provided to arrive at support systems that are suitable for highly stressed tunnels in brittle rock for civil construction and mining operations.

The primary conclusions highlight the need for improvements in better anticipating the rock mass behaviour at the tender stage and the need to design ground control measures from a perspective of practicality rather than theoretical analysis.

Specifically, with respect to excavation stability assessment, it is necessary to anticipate brittle failure processes and to properly describe the implications of shallow rock mass damage and bulking of stress-fractured ground (e.g., stand-up time reductions).

With respect to support selection, conventional support design approaches, based on standard rock mass rating systems, are severely limited in conditions where stress-driven failure processes dominate. They do not provide effective support systems for stress-fractured ground, because they do not account for mining-induced stresses, stress changes and related deformations. For tunnelling and mining at depth, it is necessary to select support systems that are effective in controlling the bulking of broken rock and able to yield when strained by deformations imposed by the stress-fractured ground. This can be achieved by following the deformation-based approach described in this article. Since rock mass bulking can impose excessive deformations that cannot be estimated by standard numerical models, it is necessary to separately estimate the deformation demand when bulking dominates (e.g., in late stage mining).

With respect to constructability, it is concluded that conditions of brittle failure must be anticipated early and thus well described in a quantitative manner in tender documents. This should include design inputs relevant for estimating stress-fracturing, for anticipating the extent of rock mass degradation and its impact on stand-up time. Most importantly, flexible and effective support systems (classes) must be provided to manage rapidly changing ground conditions and prevent related delays.

1 >> INTRODUCTION

For the economic and safe construction of deep tunnels, a contractor has to be presented with efficient and effective support systems, i.e., with flexible support classes that can be rapidly installed and are effective in managing stressfractured ground within complex geological environments and with high levels of uncertainty.

When rocks are “raining” from a finger shield and steel arches are “flying” without much contact with the rock in the tunnel roof (Figure 1), something has gone wrong and the construction process is hampered causing costly delays and rehabilitation (e.g., shotcreting through mesh and behind steel sets) and wear and tear (e.g., to conveyors).

Figure 1 illustrates such conditions, conditions that form the framework for this lecture showing: (a) stress fractured ground emerging from the finger shield, and (b) bolted u-profiles that provide little effective support due to stress-driven overbreak until the overbreak is filled by shotcreting through the mesh.

In these conditions, it is necessary to properly anticipate the actual rock mass behaviour, arrive at the most optimal excavation technique and then provide flexible but reliable means for the support of a shell of stress-damaged, broken ground. Only when this rock mass behaviour is properly anticipated can the most appropriate support classes be selected, rapidly installed and become effective in managing the stress-fractured ground such that tunnelling can proceed without unnecessary delays. In other words, an robust engineering design must not just ensure stability but also facilitate rapid and cost-effective construction. From personal experience, it seems that the later is often neglected leading to excessive costs once contractual arrangements have been made without due respect for the actual ground control challenges the contractor faces.

In the spirit of Sir Alan Muir Wood, the author hopes to make a contribution by “pushing for innovation as a key for economy and safety” (per ITA website) in deep tunnelling, particularly when “uncertainty is a feature”

(per ITA website) that must be understood by sound engineering designs; designs that respect the reality of construction and the need for workplace safety.

In this lecture, the author draws on his experience in deep mining and Alpine tunnelling where static and dynamic failure processes had to be managed as mining-induced stresses caused shallow and deep-seated rock mass failure. Based on the author’s geomechanics background, the lecture of course focuses on geotechnical design aspects. Findings from collaborative research with colleagues such as Drs M. Cai (Laurentian Uni.), E. Eberhardt (Univ. of British Columbia), M. Diederichs (Queens Univ.), E. Hoek, D. Martin (Univ. of Alberta) and many more are reflected in this article and merged with “real world” observations to draw attention to the need for engineering designs that respect the often rather limited toolbox of a contractor.

1.1 DESIGN HURDLES FOR OPTIMAL CONSTRUCTABILITY

In practice, there are several points of disconnect in the engineering design process that may eventually lead to unnecessary delays and cost overruns. Whereas this lecture deals with tunnelling at depth in hard rock, the findings are often of general nature and can be adapted to other ground conditions. The reason for this relatively narrow geomechanics focus is twofold: brittle rock mass behaviour has, in the author’s experience, lead to many unnecessary construction problems, and Canadian researchers have, over the last decades, significantly advanced our understanding of brittle rock mass behaviour.

Some challenging engineering design aspects to overcome for economic constructability are the selection of the most appropriate excavation technique (Drill and blast (D&B) versus mechanized excavation (MechEx)) and the most efficient¹ and effective² support systems. Much progress to overcome these challenges can be made by:

- better understanding and properly documenting in a quantitative manner (in



Figure 1 (top) : Rock “raining” from finger shield behind TBM and (bottom) steel arches “flying” without contact with tunnel roof (Photos courtesy: TAT consortium 2004)

¹ Efficient means facilitating rapid construction.

² Effective means providing optimal ground control.

1 >> INTRODUCTION

tender documents) the anticipated rock mass and excavation behaviour (i.e., the anticipated excavation failure modes);

- better qualifying relevant rock mass characteristics and their variability to better anticipate the range and spatial variability of potential instabilities and related support demands;
- adopting representative numerical models and inputs that capture the actual rock mass behaviour and respect the limitations of empirical methods and modelling tools; and
- accounting for practical constraints during construction by matching a design to a chosen construction process.

A robust design for constructability must facilitate the selection of excavation techniques that fits the ground over the entire project length and the selection of efficient and effective support systems for each rock mass domain.

2 >> ELEMENT OF EXCAVATION DESIGN

2.1 EXCAVATION BEHAVIOUR

The well-established excavation behaviour matrix presented in Figure 2a indicates that tunnel instability modes are controlled by three factors: the rock mass quality, the stress level, and structural features. The related consequences of different instability mechanisms and support responses are nicely reflected in the corresponding image matrix of Figure 2b prepared by Hoek (2015) from his lecture on “The Art of Tunneling”.

The horizontal axis reflects the rock mass quality and the axis on the right of the matrix in Figure 2a highlights that the stress level (SL_{UCS}) defined as the ratio of σ_{max}/σ_c , with σ_c representing the unconfined compressive strength obtained from triaxial testing according to Hoek and Brown (1988), can be used to assess the impact of stress. Since the maximum tangential stress $\sigma_{max} = 3\sigma_1 - \sigma_3$ considers both principal stress components and therefore the stress ratio $k_0 = \sigma_1/\sigma_3$, the stress level is better suited to anticipate stress-driven instability mechanisms than by only considering the overburden stress (left axis of matrix).

At low stress levels ($SL_{UCS} < 0.4$), or when extreme stress ratios cause low or negative tangential stresses in the back of excavations, structurally controlled mechanisms dominate. These can be properly anticipated by oriented drill core analyses and careful structural mapping followed by wedge-type analyses (e.g., with Dips™ and Unwedge™; codes developed by RocScience). From a support design perspective, these failure modes are properly covered by standard classification systems and rules of thumb providing appropriate bolt lengths and densities. From a construction perspective, stand-up time issues increase to the right of the matrix of Figure 2 due decreasing rock mass quality and with increasing depth due to stress-driven fracturing and shearing.

At the other extreme of the matrix, in highly stressed and very poor (sheared) ground, squeezing conditions are encountered with plastic yield of the rock mass. In the lower right corner of the matrix, soil mechanics principles with rock mass plasticity models are applicable and time-dependent, visco-plastic deformation and swelling processes often dominate the tunnel and support performance.

In between, i.e., in the gray-hatched matrix elements of Figure 2a, stress-driven failure of massive, moderately jointed or blocks of rock between open joints constitutes part of the excavation instability process. In these situations, stress-driven fracturing of rock and rock blocks combine with shear slip and block rotation depending on the level of confinement and support constraint. This lecture focuses on conditions where stress-driven rock fracturing contributes to construction problems and thus are to be considered in the engineering design.

Swelling ground conditions are not covered here and the reader is referred to Steiner et al. (2010 and 2011) offering some innovative concepts with respect to stress-induced swelling conditions. From a construction perspective, their work suggests that excavation-induced stress raisers produce preferred water flow paths and in the long run enhance the swelling potential. This suggests that protective excavation techniques can be used to minimize the swelling potential and thus improve the long-term performance of the installed tunnel support.

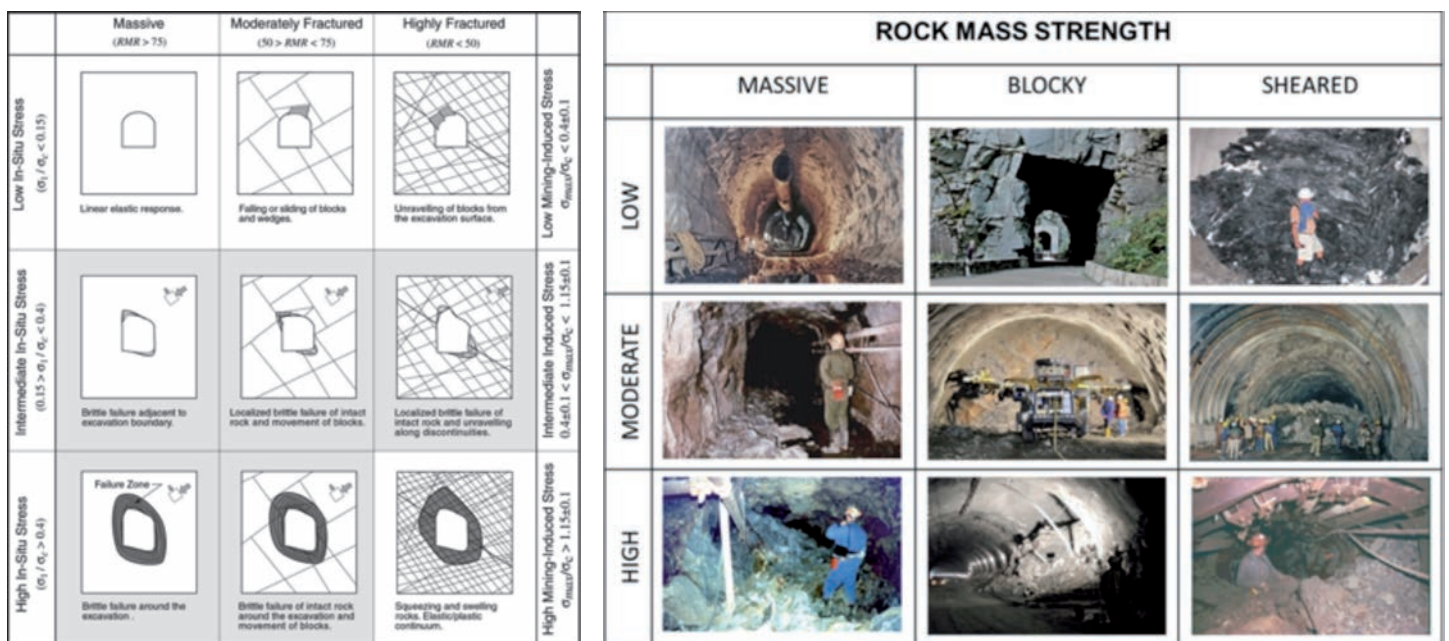


Figure 2 : Excavation behaviour matrix: (a) Tunnel instability modes (Kaiser et al. 2000); and (b) photographic representations of instability processes (courtesy: Hoek (2015) www.rocscience.com/learning/hoek-s-corner/lecture-series).

2 >> ELEMENT OF EXCAVATION DESIGN

The matrix of Figure 2 allows assigning tunnel behaviour modes to each rock mass domain along a tunnelling project. In mining, however, where the stress level is changing as the extraction ratio changes, large stopes are excavated or caves propagate, it is necessary to consider the evolution in stress level (up and/or down from a given behaviour state). For example for poor ground with $RMR < 50$ at an initial intermediate stress (right side of matrix in Figure 2a), stress relaxation may lead to structurally controlled instabilities (i.e., during unloading) followed by deep yield (i.e., upon reloading).

For the selection of the construction technique, it is necessary to assess the collective impact of all behaviour types along a tunnel. However, as Barton (2000) pointed out, even relatively short problematic sections along a tunnel (such as faults) may dominate the performance of a TBM and render it uneconomic. Aspects of excavation method selection are not covered here and the reader is referred to the work of Barton and others.

2.2 GEOTECHNICAL ASPECTS OF DESIGN PROCESS

In a most general form, the geomechanics design process to select the most appropriate excavation technique and support system for safe construction and long-term stability involves the elements described in the flow chart of Figure 3. The type of data required and the methods of design however depend largely on the anticipated rock mass behaviour and the potential failure modes. The arrows indicate locations in the design process where knowledge of the anticipated rock mass behaviour may affect or even dominate the design process. The question marks indicate that a lack of understanding of the anticipated rock mass behaviour might negatively affect the design as relevant data may not be collected and flawed empirical or numerical techniques be chosen for the design. A lack of understanding and certainly a lack of properly communicating (e.g., in the tender documents) anticipated rock mass behaviours have, as is illustrated in this lecture, often led to inefficient designs with ineffective support systems (e.g., Figure 1).

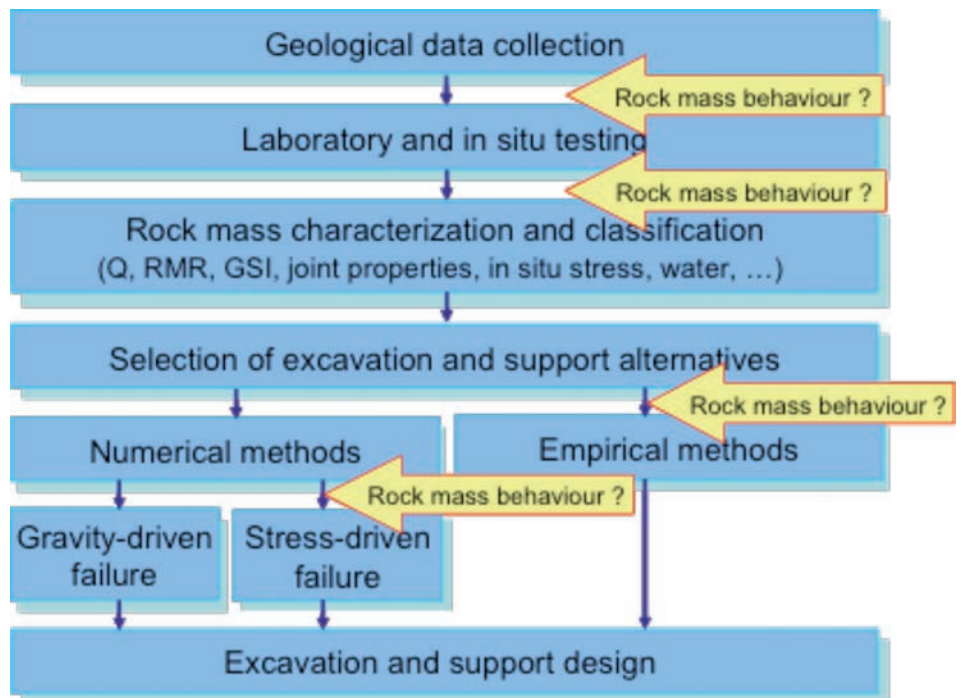


Figure 3 : Site characterization approach for standard geo-engineering projects; highlighted by arrows are locations in design process where a sound understanding of rock mass behaviour is needed (Kaiser and Kim 2008b).

In the author's opinion, too much emphasis is placed on describing the geology without direct reference to behavioural characteristics that might affect the excavation behaviour. As a consequence, standard testing programs may be conducted without focusing on the essential. Rock mass classifications may be applied to conditions that are not well suited and excavation techniques or support alternatives may be assigned that may not be suitable for construction in a well described but not properly assessed geology.

Most importantly, without a clear understanding of the anticipated rock mass behaviour, inappropriate numerical models or empirical methods may be chosen for conditions that differ drastically from reality; rendering a design less than optimal from a constructability perspective. In this sense and in the author's experience, the last arrow in Figure 3, pointing at stress-driven failure, indicates one source of greatest disconnect between desktop engineering designs and construction practice. The lack of understanding and properly communicating

the rock mass behaviour is therefore often a primary source of disconnect between engineering design and construction practice.

This is illustrated by the example shown in Figure 4a for a tunnel excavated with an open TBM (Figure 1). Brittle stress-fracturing with surface parallel fractures propagating between natural joints (photo insert) led to laterally widespread, typically between 0.5 and 1 m deep, overbreak (see insert of field mapping by geologist). For the prevailing stress condition with $k_0 < 1$ near a valley, standard numerical models using plasticity relations would point at preferential wall instability modes. However, as demonstrated by the output of ELFEN™, a Finite Element/Discrete Element fracture code by Rockfield, the predominant fracture zone moves to the roof if the tensile strength is sufficiently low. Combined with the predominant influence of gravity, this tensile fracturing then led to the less than favourable construction conditions described in Figure 1.

2 >> ELEMENT OF EXCAVATION DESIGN

Even though tensile strength results were provided in the tender documents, the most predominant tunnel behaviour mode with shallow stress-fracturing was not anticipated and support classes were prescribed that were not flexible enough to manage this ground in an efficient manner. Even though the excavation was “stable” in that the failure process was self-stabilizing, the ravelling of stress-fractured ground lead to “raining” rock and drastically affected the advance rate of the open TBM. As a matter of fact, it is retroactively evident that an early understanding of the likely and predominant failure mode should have led to the selection of a different TBM type.

2.3 QUANTIFICATION OF DESIGN INPUTS

Whereas qualitative inputs based on previous experiences often suffice, particularly in situations where past experience is fully applicable, there are several reasons for attempting to quantify the rock mass and its behaviour: to facilitate communication; to form a basis for comparison; and to provide input for quantitative design approaches (e.g., for numerical modelling or for the determination of rock loads).

2.3.1 Rock mass rating - “Putting numbers to excavation behaviour”

The need for quantification has long been recognized and Terzaghi in 1946 laid the foundation for most rating systems by defining rock classes based on blockiness, joint condition and response to tunnelling (Table in Figure 5a). The underlying failure mechanism assumed by Terzaghi was gravity-driven loading of the support (steel sets at the time; Figure 5b) and the output provided support loads. Wickham et al. (1972) introduced a quantitative method for describing the quality of a rock mass and for selecting appropriate support on the basis of their Rock Structure Rating (RSR; rating in a cumulative manner three parameter: geology, geometry, and groundwater). In the early 1970, both Bieniawski (1976; RMR) and Barton (1974; Q) independently

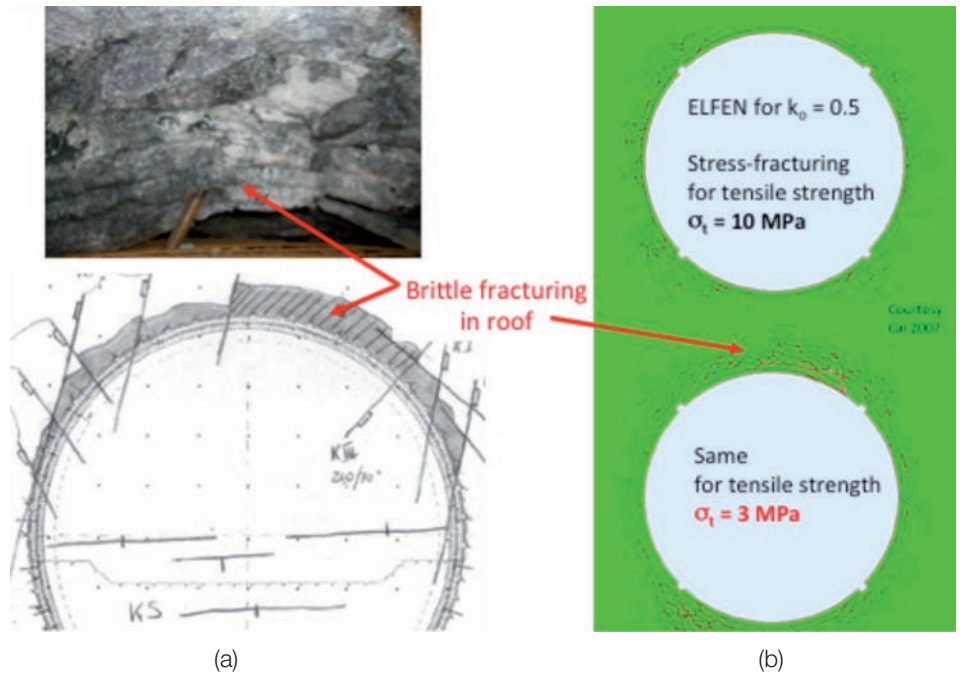


Figure 4 : Stress-fracturing involving tension or extension damage in roof of TBM excavation with $k_0 \sim 0.5$: (a) close-up of spalling gneiss and field mapping record; (b) numerical model outputs using ELFEN™ with 3 and 10 MPa tensile strength.

developed means to quantify rock mass classes, again by rating the blockiness and joint condition (and other factors such as orientation and intact rock strength for RMR; in situ stress for Q; and water for both). The data came from case studies in civil (RMR and Q) and mining applications (RMR) and the outputs of these classifications provides guidance for the selection of support systems including linings, steel sets, and/or bolts to achieve stable excavations.

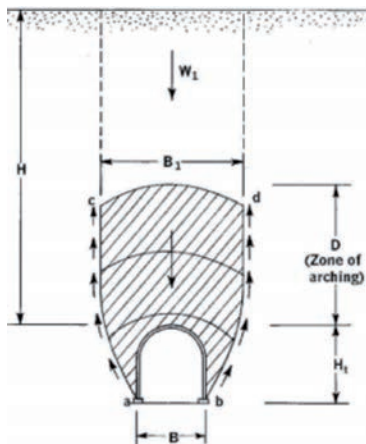
Bieniawski (1989) introduced the concept of stand-up time and provided guidance through the stability chart on the time available for support installation. From a constructability perspective, the time available for support installation before ravelling is initiated constitutes one of the most relevant aspects for tunnel construction. Unfortunately, the utility of this chart is rather limited because RMR does not account for the impact of stress; particularly not the impact of stress-fracturing (see Section 3.3).

Laubscher (1990; and Laubscher and Jakubec (2001)) recognized this and introduced a stress factor for the MRMR rating system, yet they only provided high-level guidance. By introducing the Stress Reduction Factor (SRF) the Q-system attempts to account for the impact of stress on the near excavation behaviour of a rock mass without identification of the actual behaviour modes and extent of rock mass failure. Hence, when conditions justify, the effect of stress needs to be assessed separately; e.g., by numerical modelling. The lack of quantitative means to establish rock mass strength parameters for modelling purposes provided the motivation for the development of the Geological Strength Index (GSI) described next.

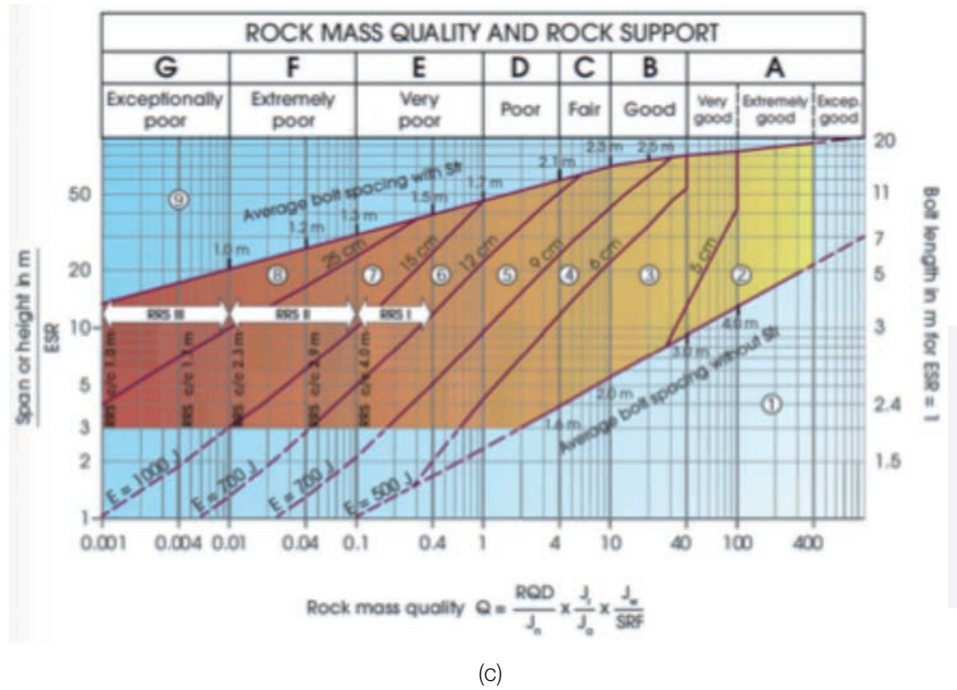
2 >> ELEMENT OF EXCAVATION DESIGN

Rock Class	Definition	Rock Load Factor Hp (feet) (B and Ht in feet)
I. Hard and intact	Hard and intact rock contains no joints and fractures. After excavation the rock may have popping and spalling at excavated face.	0
II. Hard stratified and schistose	Hard rock consists of thick strata and layers. Interface between strata is cemented. Popping and spalling at excavated face is common.	0 to 0.5 B
III. Massive, moderately jointed	Massive rock contains widely spaced joints and fractures. Block size is large. Joints are interlocked. Vertical walls do not require support. Spalling may occur.	0 to 0.25 B
IV. Moderately blocky and seamy	Rock contains moderately spaced joints. Rock is not chemically weathered and altered. Joints are not well interlocked and have small apertures. Vertical walls do not require support. Spalling may occur.	0.25 B to 0.35 (B + H)
V. Very blocky and seamy	Rock is not chemically weathered, and contains closely spaced joints. Joints have large apertures and appear separated. Vertical walls need support.	(0.35 to 1.1) (B + H)
VI. Completely crushed but chemically intact	Rock is not chemically weathered, and highly fractured with small fragments. The fragments are loose and not interlocked. Excavation face in this material needs considerable support.	1.1 (B + H)
VII. Squeezing rock at moderate depth	Rock slowly advances into the tunnel without perceptible increase in volume. Moderate depth is considered as 150 ~ 1000 m.	(1.1 to 2.1) (B + H)
VIII. Squeezing rock at great depth	Rock slowly advances into the tunnel without perceptible increase in volume. Great depth is considered as more than 1000 m.	(2.1 to 4.5) (B + H)
IX. Swelling rock	Rock volume expands (and advances into the tunnel) due to swelling of clay minerals in the rock at the presence of moisture.	up to 250 feet, irrespective of B and H

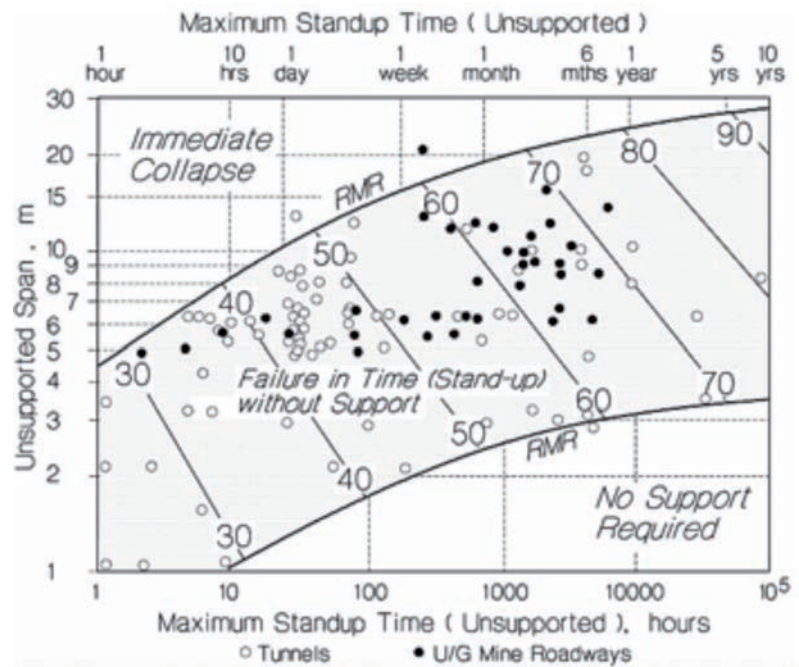
(a)



(b)



(c)



(d)

Figure 5 : Rock mass classification: (a and b) Terzaghi (1946); (c) Barton/NGI (2013); (d) Bieniawski (1984 and 1989; from Hutchinson and Diederichs (1996)).

2 >> ELEMENT OF EXCAVATION DESIGN

2.3.2 Rock mass strength characterization - "Putting Numbers to Geology"³

Three components of a rock mass need to be quantified to arrive at its strength: the strength of the homogeneous, intact rock; the strength of the rock blocks (if heterogeneous or "defected" it is less than that of the intact portion of the rock); and the condition of the block forming joints. Figure 6 illustrates these three components of a rock mass with rock blocks formed by open joints composed of cohesive defects and "intact" rock in the sub-blocks between the defects. The core image illustrates that defects may often break during drilling and, if interpreted as joints, lead to a misrepresentation of the rock mass (underestimation of ratings).

"Intact" rock strength

The strength of the homogeneous portions of a rock block, typically called the intact strength, is to be obtained by laboratory testing. Hoek and Brown (1988) recommend that the unconfined strength σ_{ci} be obtained from triaxial tests. Core damage and micro-defects often distort the results of UCS tests and the reported UCS-values are then not representative of the strength of the homogeneous portion of the rock. The mean UCS from unfiltered data may be as low as 80 to 60% of the strength of the non-defected, intact rock (Kaiser and Kim 2006). The practical implications of this are that the penetration rates may be overestimated, disk-wear underestimated and the fundamental parameter for rock mass strength determination also underestimated. Bewick et al. (2015) provides guidance for the proper determination of the unconfined rock strength.

Rock block strength

When rock blocks are defected as shown in Figure 6, rock blocks become prone to stress-fracturing and the representative strength of the defected block may be much lower than the intact strength of the homogeneous portion (the sub-blocks in Figure 6). Hoek and Brown (1988) suggested that the defected strength or rock block strength could be obtained by a

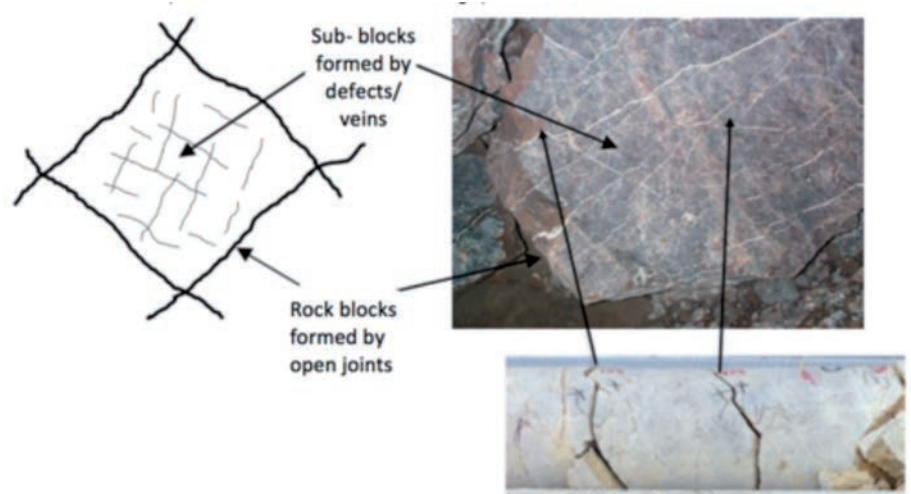


Figure 6 : Cartoon of elements of a defected rock mass: blocks formed by open joints with volumes of "intact" rock formed by defects (sub-blocks); example of a defected rock in photo from a rock mass with widely spaced open joints (scale: photo edge length 1x 1.3m (Kaiser 2016; ISRM lecture) with defects (veins) at dm-scale; core shows broken veins in drill core from defected rock blocks.

large number of tests of core and Laubscher and Jakubec (2002) provided an approach to obtain the unconfined rock block (and rock mass) strength by rating the density of defects and the hardness of the infilling. The bottom line being that the rock block strength needs to be established separately if the blocks between open joints are prone to stress-fracturing (see following section).

Rock mass strength

Laubscher recognized the impact of defects and developed the MRMR-system to obtain the unconfined rock mass strength but did not provide means to determine the confined rock mass strength.

Hoek (1999) in his lecture on "Putting numbers to Geology" discusses the need for and complications in arriving at quantitative descriptors for the rock mass quality. He describes that the design process should move from a largely qualitative preliminary assessment to a highly quantitative analysis of excavation performance and support demand for situations that require such analyses. In other words, when appropriate, empirical and semi-empirical means may have to be replaced by numerical models that capture the rock mass behaviour and the associated excavation instability

mechanisms. This challenge will be discussed below for conditions involving stress-driven rock failure.

Geological Strength Index (GSI) approach

Because none of the rock mass rating systems described above did provide, and are still not providing, reliable input parameters for numerical models, the GSI (Geological Strength Index) was developed based on the same descriptors (blockiness and joint condition) to provide a matrix to obtain the GSI. Cai et al. (2004) quantified both axes of the matrix leading to the chart presented in Figure 7.

Hoek (pers. comm.) expressed concern about the quantification of the GSI-chart as it opens the possibility for inconsiderate misuse without due respect for the underlying geological conditions. The GSI is not a precise number (at best within a range of ± 5 points) and must always be accompanied with a descriptor of the prevailing rock mass characteristics and the anticipated behaviour. For example, for a rock mass with $GSI = 60 \pm 5$, a descriptor of the rock mass may include "The rock mass contains moderately spaced, well interlocked joints that are not chemically altered" and of the anticipated behaviour "and vertical walls are

³This terminology is adopted in reference to lecture by Hoek (1999) on this topic.

2 >> ELEMENT OF EXCAVATION DESIGN

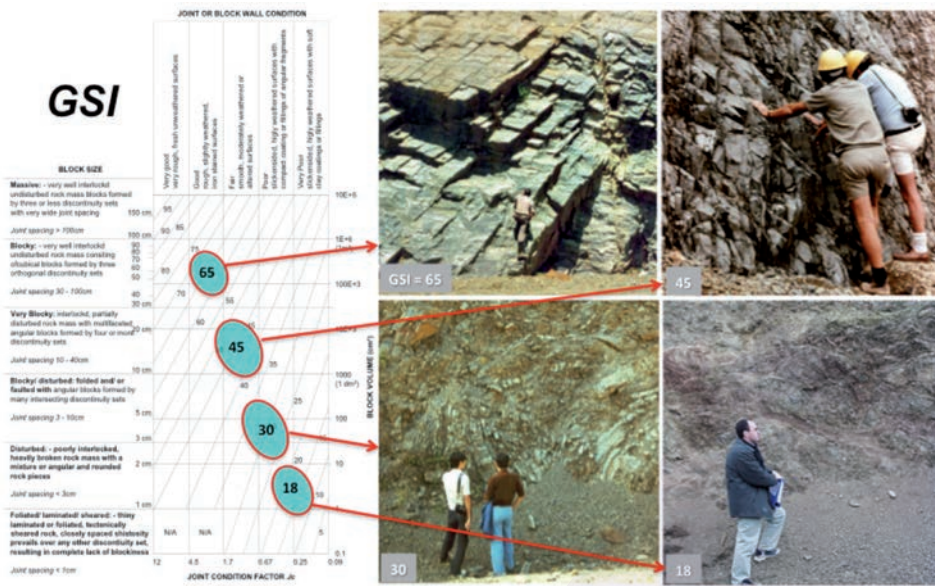


Figure 7 : GSI with quantified blockyness and joint condition (Cai et al. 2004) and four examples from lecture by Hoek (2016) on "Rock Mass Properties" (pers. com.; to be released shortly).

expected to be free standing but may spall when highly stressed"; just as Terzaghi did for the rock classes in Figure 5a (e.g., for Rock class IV).

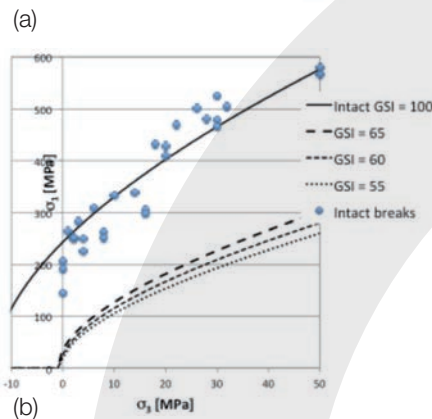
This index was then combined with the non-linear Hoek-Brown (1988) failure criterion (Figure 8a) that was established to capture the non-linear nature of the rock and rock mass failure envelopes (Figure 8b) and calibrated against limited field data but validated on observations from underground excavations in many different geological settings (primarily for GSI < 65). The GSI approach to strength determination therefore has been verified for the estimation of near excavation behaviour in rock classes of blocky to disturbed nature (illustrated by examples in Figure 7). The constants C_s and C_m given in Figure 8a are therefore only strictly valid to obtain the rock mass strength near excavations.

In the author's opinion, while far from perfect (see ISRM lecture), the GSI approach provides the only⁴ systematic means to arrive at rock mass strength parameters. Early attempts by Bieniawski were limited to coal measure rocks and recent attempts

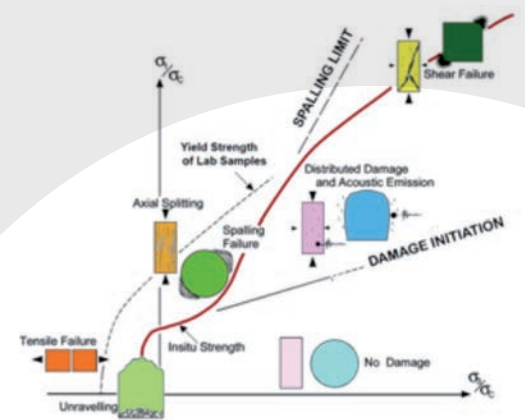
$$\sigma'_1 = \sigma'_3 + \sigma_c \left(m_b \frac{\sigma'_3}{\sigma_c} + s \right)^{0.5}$$

$$s = \exp\left(\frac{GSI - 100}{C_s - 9}\right) = 0.0067 \text{ to } 0.0117 \text{ to } 0.0205$$

$$\frac{m_b}{m_i} = \exp\left(\frac{GSI - 100}{C_m - 28}\right) = 0.201 \text{ to } 0.240 \text{ to } 0.287$$



(b)



(c)

Figure 8 : (a) Hoek-Brown Failure criteria with s and m values for $GSI = 60 \pm 5$; (b) resulting rock mass strength envelopes for intact rock data shown; and (c) s-shaped envelope differentiating between extensional and shear failure zones (Kaiser et al. (2000) and Diederichs (2003)); note: σ_c in equation is σ_{α} according to Hoek and Brown (1988) and not the average UCS.

⁴ In the author's opinion, poorly justified criticisms have recently been voiced in the European literature with accusations of lack of scientific rigor in the development of GSI and practical irrelevance for rock engineering purposes. These criticisms are frequently based on ignorance and are never supported by better-quantified alternatives. Furthermore, they are propagated to prevent means for quantitative rock mass strength determination based on fears of claims during project execution. Such fears should not be used to provide insufficient and vague information, and to ignore descriptions of anticipated failure modes.

2 >> ELEMENT OF EXCAVATION DESIGN

Furthermore, as discussed by Kaiser (2016; ISRM lecture), the GSI approach is not directly applicable for the determination of the confined rock mass strength and is limited in application to conditions where the rock blocks are formed by at least three open joint sets and the block size is less than about 1/10th of the excavation span.

For massive to moderately jointed rock masses, blocks of rock between open joints or rock bridges in non-persistent joints have to fail in tension or by shear through intact or defected rock. Hence, the GSI may not be applicable and it is necessary to establish the rock block strength. This is illustrated by the work flow in Figure 9a resulting in block strength between 80% of σ_{ci} for micro-defected homogeneous rock to 65 to 32% of σ_{ci} for heterogeneous blocks.

Once the block strength is established, the failure envelope in the low confinement zone can be obtained as shown in Figure 9b (on the left) and for the high confinement zone by the approaches shown on the right. For details, the reader is referred to Kaiser (2016; ISRM lecture).

In a somewhat simplistic manner, GSI is applicable on the right side of the tunnel stability matrix and the block strength dominates the behaviour on the left side of this matrix (Figure 10).

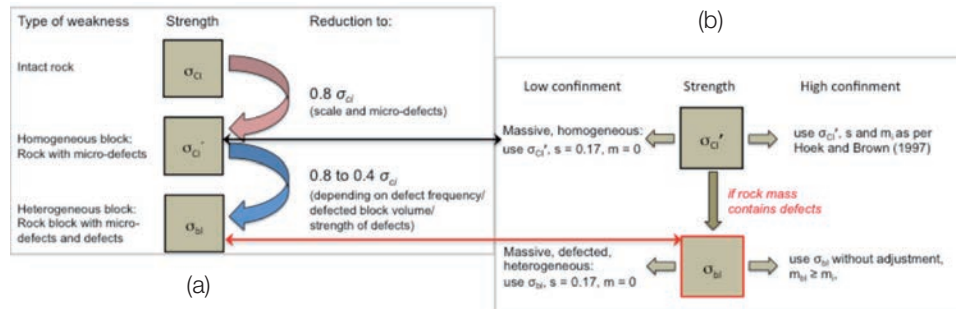


Figure 9 : (a) Adjustment process for block strength of homogeneous to heterogeneous blocks; and (b) rock mass strength determination if GSI is not applicable in massive to moderately jointed and/or defected rock.

2.3.3 In situ and induced stress

Depending on the selected data set, typical vertical stress gradients are reported as $0.0265 \pm 0.001 \text{ MPa/m}$ (e.g., Martin et al. (2003) or Herget (1988)). The horizontal stresses (H for major and h for minor horizontal stress) vary widely depending on the geological as well as the thermal and tectonic setting. The selected depth range and the adopted statistical fitting procedures heavily influence the fitted trends. Because of rock mass yield related stress relaxation effects near the surface, Maloney et al. (2006), building on findings from the

Scandinavian Shield, demonstrated that it is often necessary to separately interpret data from shallow depth (<400 m; Domain 1) and from greater depth (>600 m; Domain 3). As a consequence, reported “best-fit” stress profile equations are often practically meaningless without defining applicability limits in terms of depth range and geological setting. Furthermore, as demonstrated by Kaiser et al. (2106), rock mass heterogeneities in different geological and thermal/ tectonic settings affect the local stress field (both the variation in stress magnitude and the gradient with depth).

The effect of tectonic straining on a heterogeneous rock mass is illustrated by use of a heterogeneous Voronoi model subjected to horizontal straining (Figure 11a and b; RS2™ by RocScience). The model output (Figure 11c) shows stress variations in the order of 10 to 20 MPa in all principal stress components (these stress variations of course depend on the assumed rock mass heterogeneity). Of practical relevance is that the horizontal stress gradient at depth (typically below 600 m) is much lower than the vertical stress gradient. These findings were verified by comparison with field measurements (Kaiser et al. 2016) showing that observed, often highly variable, stress measurements reflect reality and must be considered when assessing stress-driven failure processes along a project alignment (see below).

The in situ stress field is modified by the stress flow around underground excavations. For a circular shaft, in an elastic media, the Kirsch

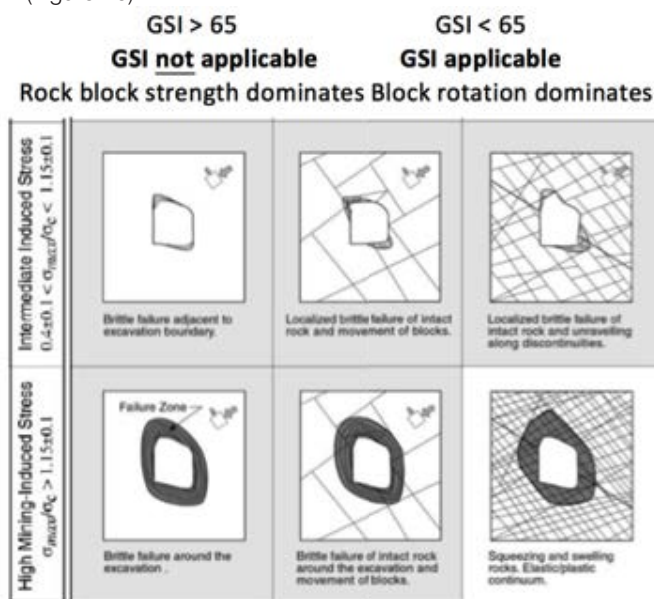


Figure 10 : Limits of applicability of GSI approach for rock mass strength determination.

2 >> ELEMENT OF EXCAVATION DESIGN

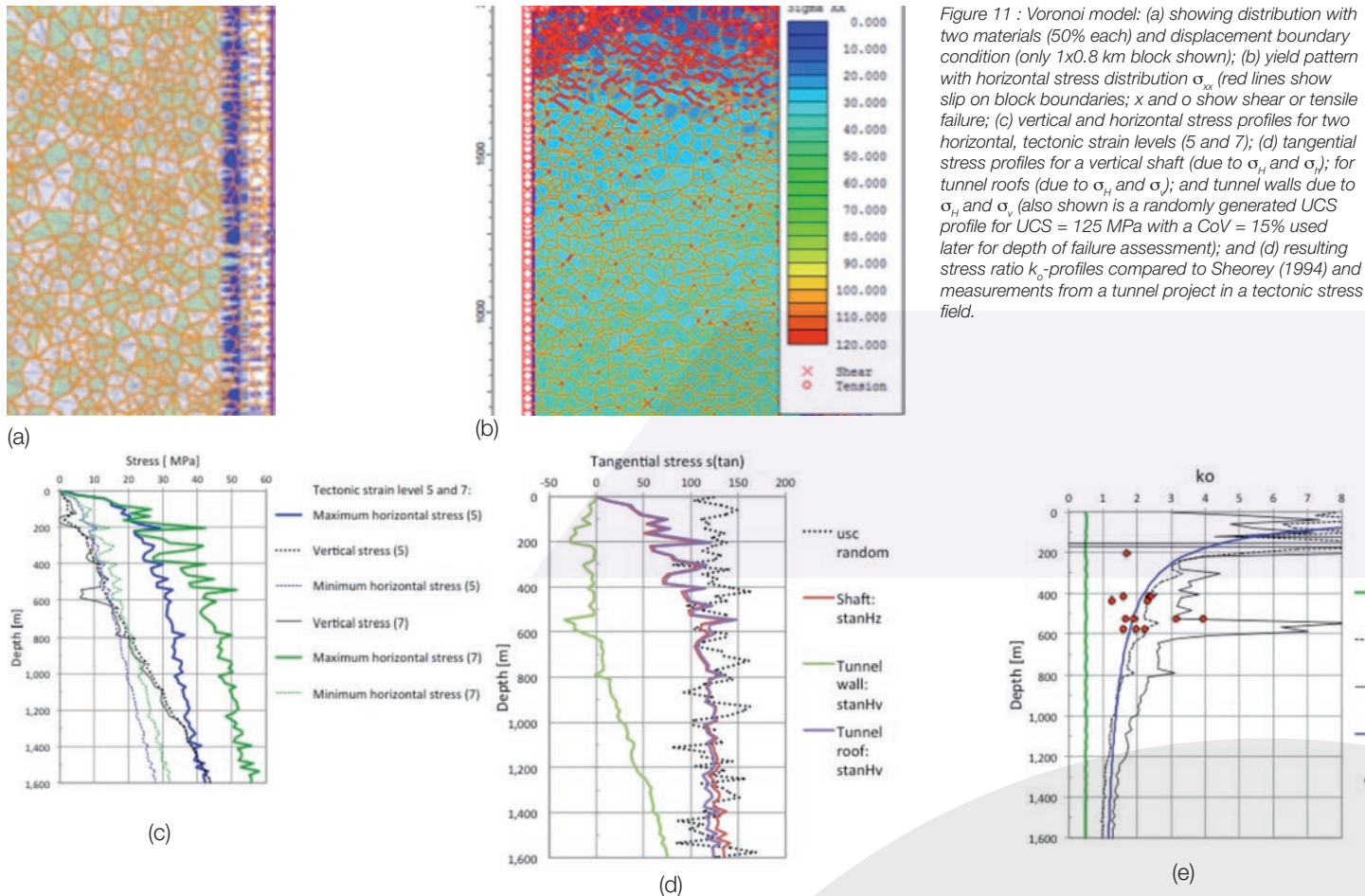


Figure 11 : Voronoi model: (a) showing distribution with two materials (50% each) and displacement boundary condition (only 1x0.8 km block shown); (b) yield pattern with horizontal stress distribution σ_{xx} (red lines show slip on block boundaries; x and o show shear or tensile failure); (c) vertical and horizontal stress profiles for two horizontal, tectonic strain levels (5 and 7); (d) tangential stress profiles for a vertical shaft (due to σ_v and σ_H); for tunnel roofs (due to σ_H and σ_v); and tunnel walls due to σ_H and σ_v (also shown is a randomly generated UCS profile for UCS = 125 MPa with a CoV = 15% used later for depth of failure assessment); and (e) resulting stress ratio k_0 -profiles compared to Sheorey (1994) and measurements from a tunnel project in a tectonic stress field.

equation produces the maximum tangential stress (σ_{\max} or $s(\tan)$) profiles for elasticrock as shown in Figure 11d (red line). Local maximum tangential stress peaks exceeding 100 MPa can be observed from shallow depths (>200 m) and local peaks reaching 150 MPa below 500 m. At greater depth the stiffness variations have less influence and the variation in induced stress becomes less variable at depth but tangential stress still varies by 10 to 20 MPa.

Also shown, in Figure 11d, are the tangential stress conditions in the roof and walls of hypothetical tunnels in the minor horizontal stress direction. Whereas the tangential stress rapidly increases and tracks the conditions anticipated for a shaft, near zero or negative minimum tangential stresses could be encountered down to 800 m. This creates potentially unfavourable overbreak conditions in blocky ground for the walls and local stress-fracturing in the roof.

The resulting stress ratio k_0 ($= \sigma_H/\sigma_v$) is shown in Figure 11e for two strain scenarios (5 and 7) together with Sheorey's model for a rock mass modulus of 80 GPa. The trend of the heterogeneous model is similar to that predicted by Sheorey but the variability in stress ratio is higher for the straining case 5 and much higher for the elevated straining case 7. This modelled variability is compared to results of a stress measurement campaign along a tunnel in a tectonic strain field (shown by red circles). For example, in the depth range 400 to 600 m, the measured k_0 ranges from 1.3 to 4 (on either side of $k_0 = 2$ predicted by Sheorey for $E_m = 80$ GPa at 500 m). The modelled k_0 is sensitive to the magnitude of the tectonic strain, the heterogeneity of the rock mass, and the stress-induced yield pattern near the surface. Even though the Voronoi model does not accurately reflect the spatial distribution of the rock

mass modulus at tunnel where the stress measurements were taken, the model and the measurements demonstrate that wide variations in stress ratio have to be expected along a tunnel even if the overburden depth does not vary widely.

From a practical perspective, Figure 11 demonstrates that a highly variable stress field must be expected along a tunnel or shaft even if the geology is relatively uniform. Except at great depths (>1500 m), the stress ratio is rarely near unity, as often suggested in tender documents, and this may strongly influence the excavation behaviour as conditions of stress-relaxation and stress-fracturing may be encountered within short distances and the location of stress-fracturing may locally rotate from the tunnel back to the walls. In underground mines with mining-induced straining, these stress variations can be magnified (not shown).

3 >> ANTICIPATING ROCK MASS BEHAVIOUR AT DEPTH

In highly stressed ground, stress-fracturing must be anticipated and the GSI system, without the modifications described above, is only applicable for conditions described by the right half of the “split” tunnel behaviour matrix presented in Figure 10. Otherwise, stress-driven rock mass damage processes have to be considered.

3.1 ROCK MASS BEHAVIOUR IN BRITTLE FAILING GROUND

Near excavations, the confining pressure is low (Figure 12a) producing an inner shell of rock that is lightly confined even when supported. If a tunnel is excavated or loaded by tangential straining during mining, stress heterogeneities cause tensile stress conditions (Diederichs 2003) in this inner shell and Griffith-like fractures can propagate and cause stress-fractures as illustrated by the bonded block model in Figure 12b and c. During excavation (Figure 12b with $k_0 < 1$), stress-fracturing starts in the roof and floor due to the elevated horizontal stress but then rapidly propagates to the walls when vertically loaded (Figure 12c; e.g., due to cave loading). This fracturing expands the low confinement zone and produces an almost circular stress-damaged inner shell (Figure 13) that will require a deformation compatible support (see section of deformation-based support design).

Continuum models with standard elastic, plastic or brittle-plastic models cannot capture this process independent of whether linear (Mohr-Coulomb) or curved (Hoek-Brown) failure envelopes are employed. Models have to be “tricked” to arrive at approximations that reflect the consequences of stress-fracturing. For example, Martin et al. (1999) provided brittle Hoek-Brown parameters to estimate the depth (but not lateral extent) of failure and Diederichs et al. (2010) stipulated a means to respect the fracture initiation threshold at low confinement as well as the transition to shear behaviour at high confinement. For this purpose, they simulated the failure process in a continuum model with a cohesive peak and a mostly frictional residual envelope that exceeds the peak envelope near the inner/outer shell transition (called spalling limit; Figure 13). This double-envelope approach can be incorporated through appropriate specification of the “peak” and “residual” parameters (e.g., in RS2™ by RocScience) or as strain-dependent mobilization of cohesive and frictional strength parameters (e.g., in FLAC by Itasca).

From a practical perspective, and by combining Figure 8c and Figure 12a, it follows that various engineering problems can be assigned to inner shell dominated behaviour (Figure 13 left) such as:

- support design; stand-up time or cave propagation; slaking or brittle failure induced swelling; strainbursting and stress-induced fragmentation;

or to outer shell dominated behaviour (Figure 13 right) such as:

- pillar design; pillar burst potential assessment; and abutment strength evaluations.

This separation in behaviour modes has long been recognized in deep South African mines where shear failure is detected ahead of an advancing stope and spalling-type failure near the stope face (Spottiswoode et al. (2008)

3.2 DEPTH OF FAILURE IN STRESS-FRACTURED GROUND

A semi-empirical approach for the determination of the extreme depth of failure in stress-fractured or spalling ground was presented by Martin et al. (1999; Figure 14a shows the normalized radius of failure versus the stress level ($SL_{UCS} = \sigma_{max}/UCS$) normalized to UCS). Diederichs et al. (2010) plotted the same information against an alternate definition of the stress level SL_{CI} by normalizing the maximum tangential stress to CI (the Crack Initiation stress) and added some additional data (Figure 14b). The additional data confirms the trend established by Martin et al. (1999). It is important to recognize that the data points plotted on these figures reflect extreme cases, i.e., the deepest observed depth of failure recorded for a given geological and stress domain. This extreme depth of

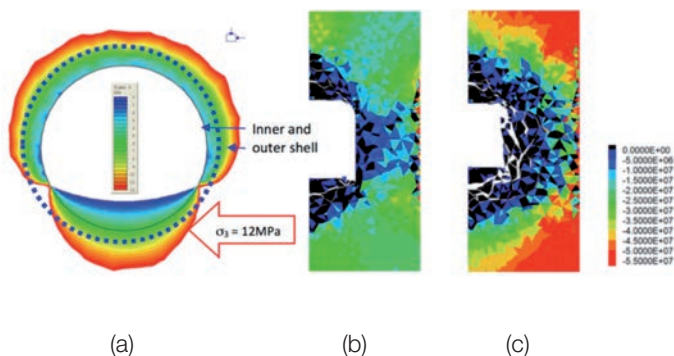


Figure 12 : (a) Minor principal stress contours (range: 0 - 12 MPa) around excavation in elastic rock for $k_0 = 0.75$; (b) Minor principals stress evolution in Bonded Block Model (BBM in 3DEC; courtesy Itasca Ltd).

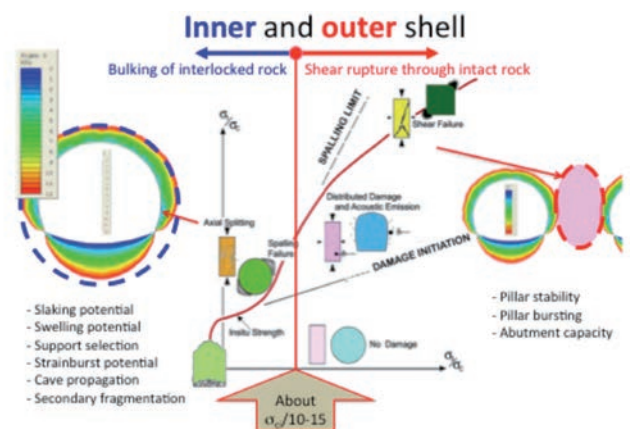


Figure 13 : Assignment of engineering problems to inner and outer shell stress space of Figure 8c (see text for explanation).

3 >> ANTICIPATING ROCK MASS BEHAVIOUR AT DEPTH

failure d_f normalized to the tunnel radius a is described by: $d_f/a = 1.25 SL_{UCS} - 0.51$.

If it is assumed that the estimated depth of failure along a tunnel follows a normal distribution⁵ (as super imposed on Figure 14a for $SL_{UCS} = 0.75$), about 40% of the tunnel would not experience any failure, 50% would experience a depth of failure of less than 8% of the tunnel radius (or 0.04 m for $r = 5$ m) and 5% or less would experience a depth of failure greater than 47% of the tunnel radius (or >2.4 m for $r = 5$ m).

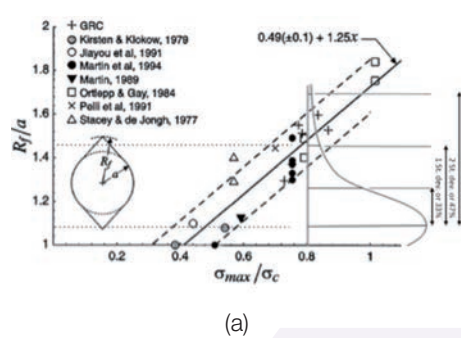
Recent work by Perras and Diederichs (2016) indicates that the trend is non-linear, suggesting that the linear trend line may overestimate the depth of failure for elevated stress levels ($SL_{UCS} > 1$). More importantly, they established a means to estimate three levels of stress-driven rock mass damage: the mean depth of failure (called HDZ; full red line for a granitic rock), the mean depth of visible damage (called EDZ_i; dashed red line); and the depth of micro-damage (called EDZ_o; red dash-dotted line). The first (HDZ) is relevant for civil and mining construction, the later two for sealing of nuclear waste disposal sites. The mean normalized depth of failure is approximated for the following discussion by the blue dashed line described by: $d_f/a = 0.35 SL_{UCS} - 0.15$.

The practical relevance of this figure for tunnel construction is that:

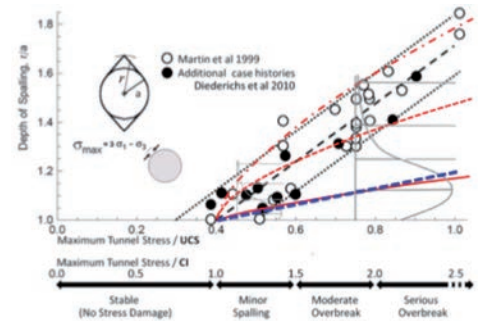
- spalling starts at about 42% of the rock's UCS (at $SL_{UCS} = 0.42$) or at the crack initiation threshold CI;
- the mean depth of failure exceeds 20% of the tunnel radius (or 1 m for $r = 5$ m) when the maximum stress reaches the UCS; i.e., for the granitic rock type when $SL_{UCS} = 1$; and
- the extreme depth of failure reaches about 80% of the tunnel radius (or 4 m for $r = 5$ m) when the maximum stress approaches the UCS.

This explains the widespread stress-damage experienced at the Bodio lot while tunnelling in gneissic rock during the advance of the St. Gotthard tunnel (see earlier; Figure 4).

For mining applications, Kaiser and Kim (2008b; based on Kaiser et al. (1996)) provided modified extreme depth of failure equations for excavations experiencing dynamic loading from seismically induced ground motions.



(a)



(b)

Figure 14 : Depth of failure charts in terms of radius of failure: (a) modified after Martin et al. (1999) with depth of failure distribution added; and (b) Diederichs et al. (2010) with normal distributions added and with damage limits for granitic rock according to Perras and Diederichs (2016) superimposed (see text for description).

3.3 STAND-UP TIME IN ROCK MASSES WITH STRESS-DRIVEN ROCK MASS DEGRADATION

Stress-induced rock mass degradation reduces the rock mass quality, primarily in the inner shell where stress-fracturing is prominent. This is illustrated by Figure 15 showing four examples of stress-driven failure of excavation walls or backs together with the related path in the GSI chart (Figure 15a):

- Piara exploration tunnel excavated in two types of gneiss by TBM in Switzerland (Figure 15b);

- Löttschberg tunnel excavated in granite, granodiorite and gneiss by TBM in Switzerland (Figure 15c);
- URL in Pinawa, Canada, excavated in granite by protective parallel hole drilling (Figure 15d); and
- Beaconsfield mine in Quartzite excavated by drilling and blasting (damage caused by seismic event) (Figure 15e).

In all cases, the rock mass in the inner shell was degraded by stress from an initially very good quality rock (with $GSI > 65$) to heavily damaged rock with GSI as low as 50 to 35.

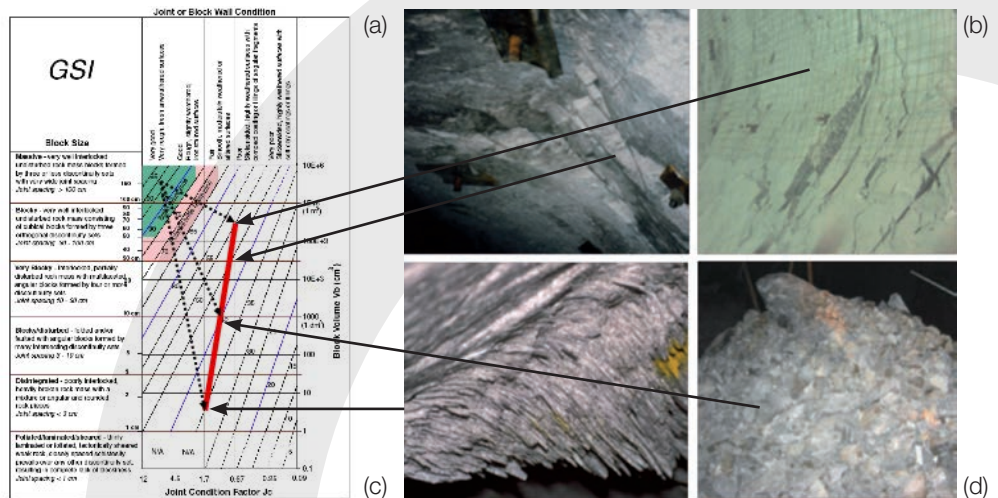


Figure 15 : (a) GSI-chart showing degradation paths for ultimate block sizes of 700, 100 and 15 mm edge lengths for: (b) spalling in back of Piara tunnel (image ~2 m wide); (c) Löttschberg tunnel wall (slab about 30 cm thick); (d) Spalling in notch at URL, AECL, Canada (image about 1 m wide); and (e) fragmented fall of ground due to rockburst (image about 2.5m wide).

⁵ Note: zero depth of failure corresponds to situations that are marginally stable ($FS = 1$); negative calculated depth of failure values of course are not possible but indicate situations of zero depth of failure with a safety margin, i.e., with $FS > 1$ for stress-fracturing.

3 >> ANTICIPATING ROCK MASS BEHAVIOUR AT DEPTH

The related impact of this degradation is highlighted in Figure 16 showing the degradation path in Bieniawski's stand-up time diagram (Figure 16a; for a 5-10 m unsupported span) and the corresponding times in the GSI chart of Figure 16b. The rock mass degradation pushes the stand-up time to near zero values and constructive measures (near face support) are required to prevent overbreak or to stabilize broken rock (prevent "raining" rock).

From a construction perspective, the potential for and timing of instability mechanisms have to be identified early, i.e., during the tender stage for the selection of the most appropriate excavation technique (D&B versus MechEx) and for the establishment of efficient and effective ground support classes that facilitate an optimal execution of the chosen construction technique.

3.4 ROCK MASS BULKING

If rock is blasted, the volume of the blasted rock is about 30 to 40% larger (swell factor of 1.35 to 1.45)⁶. When rock is fractured in the wall of a tunnel due to wall parallel (tangential) straining, this volume increase results in a unidirectional wall deformation as conceptually illustrated by Figure 17a and b, and would lead to a unidirectional bulking factor (BF = $\Delta l/l$) of 30 to 40%. In other words, if the depth of failure were 1 m deep, free bulking would lead to 0.3 to 0.4 m wall deformations (or floor heave). Fortunately,

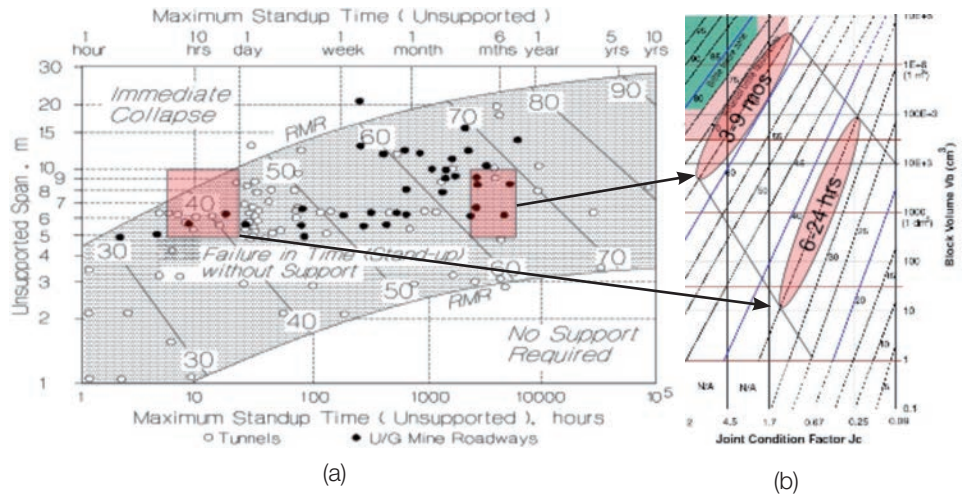
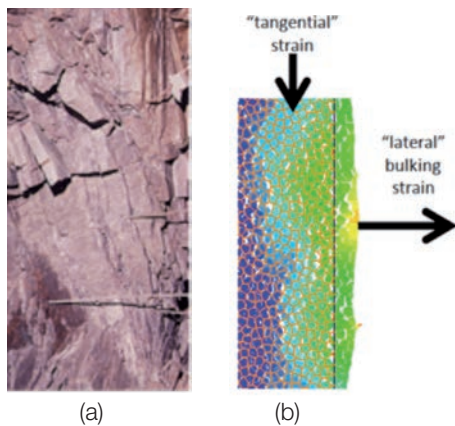


Figure 16 : (a) Stand-up time graph after Bieniawski (1989; from Hutchinson and Diederichs 1996) showing short- and long-term stability ranges for 5 to 10m wide excavations; and (b) GSI chart with corresponding characteristics for 6-24 hours and 3-9 months unsupported stand-up time.

this bulking can be significantly reduced by rock reinforcement (bolting) and confining pressure (shotcrete) as illustrated by Figure 17c. This graph shows that the bulking factor decreases rapidly with increasing radial pressure and drops to near zero values when the radial stress inside the rock mass reaches 10 to 20 MPa. Such pressures, however, cannot be provided by support alone. The radial stress (or σ_3), however, increases rapidly in the supported ground and particularly in the elastic rock beyond the stress-fractured ground (Figure 12a). In other words, the rock mass' self-supporting capacity must be mobilized by preventing raveling and rock block separation.

Most importantly, as Figure 17c shows, the amount of rock mass bulking depends on the tangential strain imposed on the rock in the inner shell. Bulking factors for three tangential strain levels are shown with an anticipated range of variability. This graph shows that much more bulking deformation must be expected in mining situation where post-excavation straining occurs, e.g., when pillar cores yield at elevated extraction ratios. As a rule of thumb, during the development of single tunnels, 2-3% linear bulking can be expected near the tunnel wall for stress-fractured rock with light support (or 20-30 mm per meter of failed rock). If the wall tunnel is more strained (by 1-2%) in the

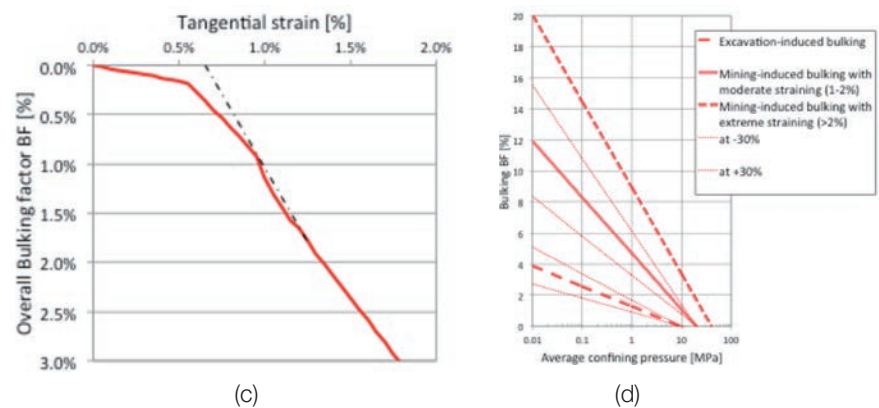


Figure 17 : Illustration of bulking process driven by tangential straining of stress-fractured rock: (a) photo of stress-fractured rock that was massive to moderately jointed (see lower corner of photo); (b) schematic tangentially strained Voronoi model with elastic rock blocks to simulate extreme geometric bulking (coloured by increasing displacement magnitude from blue to orange; zero displacement boundary on pillar side (left)); (c) relation between tangential and lateral or radial strain; strain ratio 1:3 is indicated by the dash-dotted line; and (d) recommended bulking factors for the estimation of bulking deformation as a function of confining pressure (support pressure at the wall or radial pressure imposed by the reinforced rock mass).

⁶The edge length of a volume of 1 m³ would increase by 10 to 12 %. In a tunnel, however, bulking can only occur in the radial direction and the unidirectional bulking factor BF is 35 to 40% if all but one side is restrained.

3 >> ANTICIPATING ROCK MASS BEHAVIOUR AT DEPTH

tangential direction (e.g., due to pillar yield between tunnels), 6-10% linear bulking (or 60 to 100 mm per meter of failed rock) can be expected. These values of course depend on the fracture geometry, the rock block strength and many other factors. They have been found to give a preliminary indication of the amount of deformation that can be attributed to bulking alone.

From a practical perspective, this rule of thumb illustrates that the stress-fractured ground will impose relatively large strains and deformations on the support system. During the development of single tunnels, bulking of stress-fractured rock alone will bring bolts to and beyond the yield point (if the support is installed before bulking occurs). When the strain in the tangential direction reaches 1-2%, bolts can be expected to reach their tensile capacity due to bulking alone (still leaving a safety margin of two in terms of strain to failure for typical bolt types).

3.5 VARIABILITY AND ITS IMPACT ON EXCAVATION STABILITY

The elaborations of the previous sections have shown that stress-fracturing must be expected when the tangential stress near an excavation exceeds about 40% of the rock's UCS and that the extreme depth of failure increases rapidly to about 80% of the tunnel radius when the tangential stress reaches the UCS ($SL_{UCS} = 1$). It is also shown (Figure 16) that stress-fracturing reduces the rock mass quality in the inner shell immediately around the excavation, decreasing the stand-up time to near zero values. Furthermore, rock mass bulking in the stress-fractured zone causes substantial deformations that need to be managed by the timely installation of support.

From a practical perspective, it follows that conditions with stress-induced rock mass fracturing cause highly unfavourable conditions for tunnel construction: raveling ground leading to "raining" rock, and overbreak with irregular tunnel profiles leading to "flying" arches (Figure 1). Even if the depth of failure is of a rather limited extent, say 10 to 20% of the tunnel radius (or 0.5 to 1 m in a 10 m wide tunnel), these

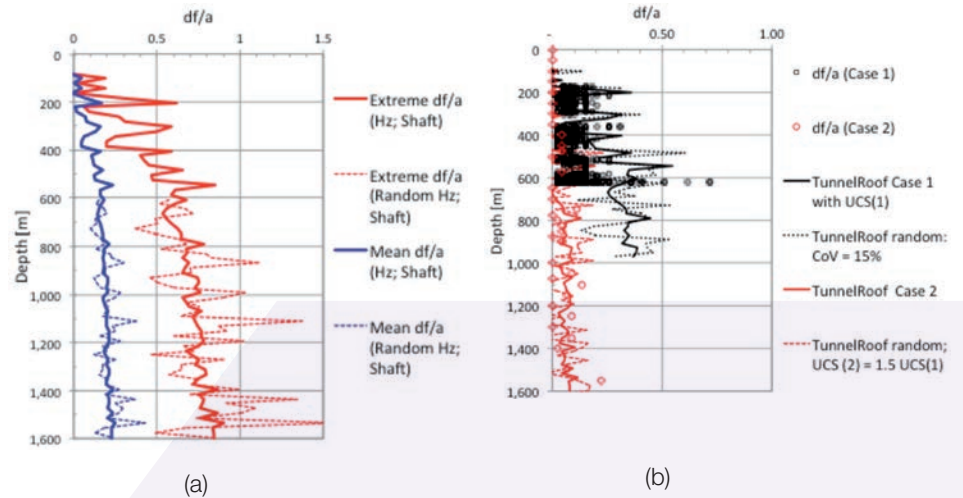


Figure 18 : Depth of failure profiles for a shaft and for tunnels at various depths (for the in situ and induced stress profiles presented in Figure 11 and the semi-empirical depth of failure relation shown in Figure 14a): (a) Shaft: estimates of mean depth of failure (for granitic rock; Figure 14b) shown in blue and extreme depth of failure with constant UCS (full red line) and with random UCS (CoV = 15%) below 600m (red dashed line); and (b) Tunnels: two tunnel cases (a shallow (<600 m; black squares) and a deep (>2000 m; red circles)) tunnel with estimated extreme depths of failures (in 50% and 125% stronger rock) with constant UCS and with CoV = 15%.

negative rock mass behaviours can cause major construction delays and increased costs if inappropriate excavation techniques and support classes are prescribed.

This rock behaviour, even in otherwise relatively uniform geological domain, can be highly variable as the stress and strength and thus the stress level (SL) change. The practical consequences of typical variability in stress and strength are explored in the following section. The variability in in-situ and excavation-induced stresses alone was already discussed in Section 2.3.3 and by Kaiser et al. (2016).

3.5.1 Variability in depth of failure

By assuming a typical fluctuation in UCS as shown in ($UCS = 125 \pm 19$ MPa (std. dev.)) and a fluctuation in local stress as described by Figure 11c, the depth of failure profiles for a shaft were produced for mean and extreme depths of failure (Figure 18a).

For the shaft, the combined effect of stress and strength variability creates a relatively narrow range in the mean depth of failure

(Figure 18a, about 0.1-0.2a or 0.3-0.6 m for $a = 3$ m) but a rather wide range in the variability of the extreme depth of failure (Figure 18b, ranging from 0.5 to 1.5-times the radius of the excavation (or 1.5 to 4.5 m for $a = 3$ m).

For two tunnels, the observed normalized extreme depth of failure is presented in Figure 18b and compared with the predictions of the model introduced in Figure 11. For the shallow tunnel (<600 m), the observed as well as the simulated normalized depth of failure range from 0 to 0.6, except for one point) with a comparable frequency of occurrence. For the deep tunnel, the observed as well as the simulated normalized depth of failure range from 0 to 0.25, again with a comparable frequency of occurrence. Even though this model does not reflect the spatial distribution⁷ at the two sites, it shows that the simulated variability in the magnitude of the extreme depth of failure corresponds well with the field observations.

⁷ The model does not reproduce the location of overbreak, as no attempt was made to match the spatial pattern of the stiffness heterogeneities, but it does reflect the variability in extreme overbreak that is to be expected.

3 >> ANTICIPATING ROCK MASS BEHAVIOUR AT DEPTH

Case example – Piora Exploration and Löttschberg tunnel (Switzerland)

The photo in Figure 1 shows stress-driven failure at the Bodio lot of the St Gotthard tunnel, Figure 15c illustrates the spalling conditions at the Löttschberg tunnel and Figure 19a at the Piora exploration tunnel. The latter case is discussed here in more detail.

Figure 19b shows an apparent non-fit of filed observations with the trend line (introduced in Figure 14). Kaiser and Kim (2006) attributed this to a lack of proper in situ stress input. After consideration of a revised k_0 -profile, consistent with the north-south tectonic straining, i.e., with k_0 decreasing from 1.5 at the portal to 0.8 at 3 km from the valley wall, the depth of failure data became concentrated around a $SL_{UCS} = 0.55 \pm 0.05$ (Figure 19c left).

The corresponding cumulative df/a distribution curve is shown on the right of Figure 19c, indicating that about 30% of the tunnel experienced stress-driven failures. The cumulative distribution curve at the Piora tunnel (red squares) is very similar to the extreme df/a distribution reported by Rojat et al. (2008) for the Löttschberg tunnel (black circles). For the Piora tunnel, an extreme $d_f/a = 0.16$ or 0.4 m for $a = 2.5$ m was predicted but locally much higher values, as high as $d_f/a = 0.6$ or 1.5 m were recorded. In both cases, the extreme d_f/a exceeded the predicted depth (using Martin et al. 1999) along about 10% of the tunnels (dashed arrow).

The practical implication with respect to constructability is that the magnitude of stress-driven overbreak and its variability can be reasonable well predicted by considering both the variability in rock strength and in in situ stress. It is also possible to estimate the percentage of tunnel length that might experience stress-driven overbreak. The location of such overbreak however cannot be predicted due to a lack of sufficient accuracy in spatial information about stress and strength. Hence, efficient excavation techniques and effective ground control measures must be selected to manage stress-driven failure processes over the entire length of tunnel where $d_f/a > 0$ is expected; i.e., when the SL_{UCS} exceeds 0.4 in brittle failing ground.

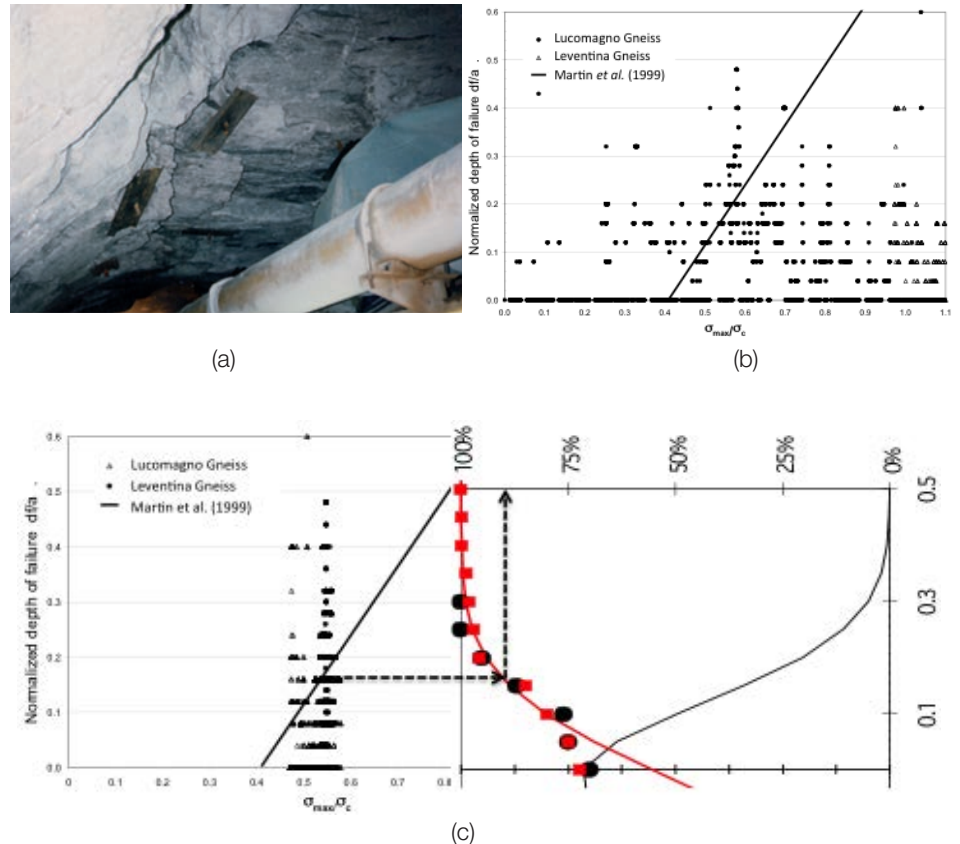


Figure 19 : (a) Photo of stress-driven overbreak at Piora Exploration Tunnel, Switzerland; (b) normalized extreme depth of failure records assuming a constant UCS, stress ratio k_0 and overburden stress (Kaiser and Kim (2006)); and (c) same after correction of changes k_0 -profile (k_0 decreasing from >1.5 near the portal to 0.8 at 3 km from portal). Also shown in (c) are the rotated corresponding probability function and the cumulative distribution curves for the Piora tunnel (red squares) and for the Löttschberg tunnel (black circles) (Rojat et al. 2008).

⁷ The model does not reproduce the location of overbreak, as no attempt was made to match the spatial pattern of the stiffness heterogeneities, but it does reflect the variability in extreme overbreak that is to be expected.

4 >> DEFORMATION-BASED SUPPORT SELECTION FOR STRESS-FRACTURED GROUND

In the following, support selection issues encountered when advancing excavations in virgin ground and when impacted by mining-induced stress-changes and related deformations are considered.

4.1 GROUND REACTION CURVE

The rock-support interaction concept or ground reaction curve (GRC) was, to the author's knowledge, first introduced by Rabcewicz (1969) and since then used by many to describe the support response to loading by excavation-induced rock mass deformations. This concept is expanded here for situations where rock mass bulking and mining-induced stress changes enhance the ground deformations.

4.1.1 GRC during tunnel development stage

When rock is excavated during the advance of a tunnel, elastic and non-elastic deformations increase as the tunnel face advances. This is illustrated in Figure 20 by three (blue) ground reaction curves showing tunnel wall deformations as a function of a fictitious internal (support) pressure for elastic (dotted), plastic (dashed) and plastic plus bulking (continuous line) ground.

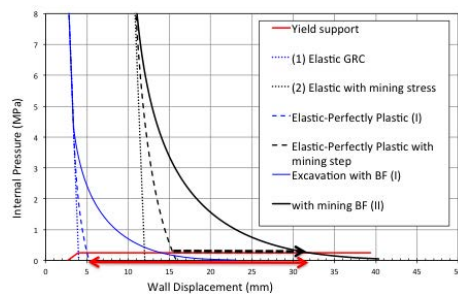


Figure 20 Ground reaction curve with convergence or wall displacement versus support pressure for a given set of engineering parameters (elastic, plastic and bulking ground in blue). Yielding support with a high yield capacity of 0.5 MPa is also shown (red). In black: Ground-reaction curves after a mining-induced, far-field stress change from 27 to 54 MPa. Black dashed arrow shows deformation increment due to mining and double arrows show total deformation imposed on support by bulking ground.

For this example, the equilibrium for plastic ground without bulking would be reached after 5 mm total deformation and with bulking after 14 mm of total deformation (25 mm without support). For a support installed at the face after 3 mm, the deformation imposed on the support would be 2 and 11 mm without and with bulking, respectively. For this case, with bulking parameters representative of a strongly bulking ground, the deformation experienced by the support would therefore be about 5-times larger than without bulking.

This suggests that bulking deformations may dominate the support behaviour and a support in bulking ground should be selected considering deformation-based design principles introduced later.

4.1.2 GRC during mining stages

Yield zone and confining pressure evolution

Mining-induced stress changes, e.g., due to loading and unloading during the advance of an undercut in a caving operation, can cause an expansion of the yield zone surrounding a tunnel with a related change in confinement (σ_3) field.

In the following figures yielding is represented by (x) for failure in shear and by (o) for failure in tension. The σ_3 -contours are shown for a range of 1 (blue) to 10 MPa (red). These contours emphasise areas:

- where the radial or confining pressure is less than 1 MPa⁸ (white to blue), i.e., where support is needed to maintain the coherence of stress-fractured rock mass; and
- where the confinement is > 10 MPa (red to white), i.e., where the rock mass is sufficiently confined to typically prevent tensile stress-fracturing and ravelling ground.

A stress path with loading of a tunnel from 30 (excavation stage) to 60 MPa deepens the shear (x) yield zone to about 2 m (compare Figure 21a and b). This loading has little impact on the depth of tensile failure (o) and on the depth of elevated confinement (location of 10 MPa contour).

Upon unloading to 15 MPa (Figure 21c), however, the low confinement zone (<1

MPa; white before blue) and the related tensile fracturing zone more than double in depth and the high confinement zone is pushed out to >3 m whereas the yield zone deepens only slightly to about 2.5 m. This drastic change in confinement contours upon unloading is of two-fold practical relevance:

- the zone prone to ravelling (<1 MPa) of stress-fractured ground is deepened by more than 100%, demanding good retention and longer reinforcements; and
- the zone of low confinement with potentially high bulking has more than doubled. As discussed below, this causes a significant shift in the GRC.

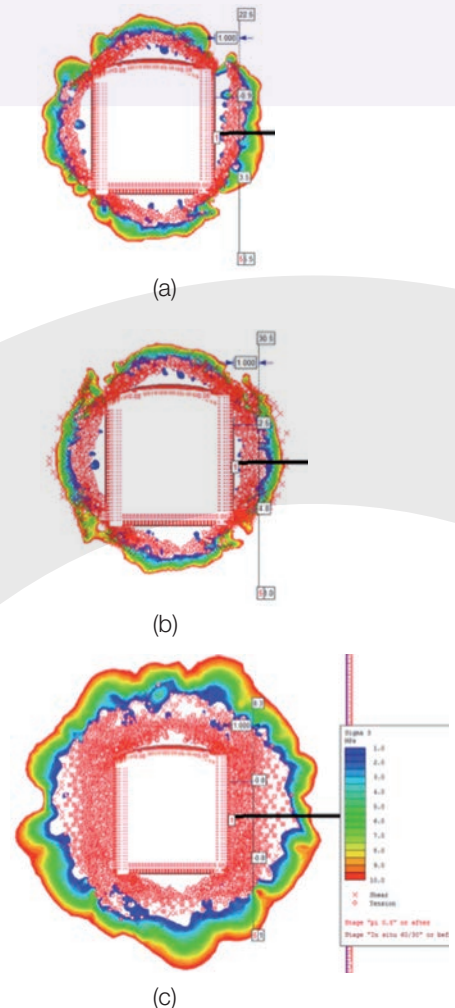


Figure 21 Yield zones and confining pressure contours for three vertical load stages: (a) after excavation at $p_v = 30$ MPa; (b) after loading to a vertical stress $p_v = 60$ MPa; and (c) upon vertical unloading to $p_v = 15$ MPa (RS2™ model; RocScience).

⁸ The area inside 1 MPa contour basically defines the zone where tensile failure dominates.

4 >> DEFORMATION-BASED SUPPORT SELECTION FOR STRESS-FRACTURED GROUND

Garza-Cuz et al. (2015) simulated the propagation of the stress-fractured zone and related deformation using a bonded block model (3DEC), also showing a rapid evolution of the stress-fractured zone upon unloading with a related zone of high bulking near the excavation.

Ground reaction curve evolution during mining

As a consequence of mining-induced stress changes, the tunnel and the rock mass surrounding the tunnel are further deformed (after excavation) causing a shift of the GRC to the right as illustrated in Figure 20 (by about 4 mm for the case shown with a far field stress increasing from 27 (blue) to 54 MPa (black)). If the support was installed at the face while tunnelling at 27 MPa field stress, an additional 7 mm of deformation (shift of blue to black GRCs) is imposed. Because the depth of yield and the related plastic deformations also increase, the total deformation imposed on the support increases to 14 and 30 mm without and with bulking, respectively (i.e., 100% and 30% higher support deformations than during the initial drive of the tunnel). The red double-sided arrow in Figure 20 indicates the total bulking related deformations imposed on the support due to the doubling of the field stress.

In summary, these ground reaction curves reveal a most important and often ignored fact that may dominate a support design; i.e., mining-induced stress changes may add substantial deformations to those experienced during the drift advance, particularly if the ground is prone to bulking. This reinforces the earlier conclusion that bulking deformations may dominate the support behaviour and that support in bulking ground should be selected considering deformation-based design principles. Stiff and brittle support rings of limited capacity, if installed before the mining-induced bulking occurs, may suddenly fail due to bulking of stress-fractured ground behind the support (potentially with a release of energy stored in the support). The support may “burst” even if the rock mass is not failing in a dynamic manner.

With respect to support design, it is important to account for mining-induced deformations that are magnified by the bulking process. This has two practical consequences:

- the rock mass bulking behaviour during tunnel advance is not representative of the future behaviour during mining, and, as a consequence, the support performance during tunnel advance is rarely representative of its behaviour during future mining; and
- the support should be designed to minimize the bulking process and thus the bulking deformation, e.g., by minimizing the post-installation deformations by rock mass reinforcement.

The later requires two actions:

- reinforcement of the broken rock such that it cannot bulk easily; and
- control the straining of the broken rock, i.e., by minimizing the tangential strain in the wall that causes the bulking.

4.2 SAFETY MARGINS FOR SUPPORT DESIGN

As in all engineering, the safety margin or risk of failure is assessed and measured by either a Factor of Safety (FS) or a probability of failure. For support design, three factors of safety are to be assessed with respect to the load, displacement, and energy demands:

$$FS_{Load} = \frac{\text{Support Load Capacity}}{\text{Load Demand}}$$

$$FS_{Disp} = \frac{\text{Support Displacement Capacity}}{\text{Displacement Demand}}$$

$$FS_{Energy} = \frac{\text{Support Energy Capacity}}{\text{Energy Demand}}$$

The goal of support in brittle failing ground is to mitigate both the cause for and the potential consequences of deformation and it follows that safety in terms of displacement demands, under anticipated static and seismic/dynamic loading conditions, constitutes the foremost design criteria. The displacement demand is controlled by the effective span of the opening, the depth of failure and the bulking factor of the fractured rock.

The support selection is then based on the load–displacement characteristics (capacity) of individual support components and the overall support system, consisting of compatible support elements to provide the desired support roles. Since the support can also affect the rock behaviour, the support selection must consider the impact of the support in an iterative manner. For example, a rebar may reduce bulking, thus reducing the strain demand on the support, but it may also strengthen the reinforced rock mass, attracting load and rendering it burst prone. A balance needs to be found between such counterproductive effects.

Of course, once a support system is designed to survive anticipated deformations it is necessary to check whether it also provides a sufficient margin against load and energy demands.

4.3 LIMITATIONS OF SUPPORT DESIGN TOOLS FOR DEFORMATION-BASED DESIGN

The above-described effect of mining and bulking, adding substantial deformations to the rock and the support, can severely limit the validity and accuracy of available support design tools; tools that have been developed for tunnelling projects (e.g., in civil engineering) that do not experience large bulking or mining-induced deformations.

For example, empirical rock mass rating systems (e.g., RMR and Q) were primarily developed for the purpose of classifying the ground for rock support selection. The underlying database however largely stems from scenarios where little bulking or mining-induced deformation was experienced⁹. These cases are not representative for conditions with heavily stress fractured ground and in mining operations experiencing loading, unloading and reloading cycles.

The Geological Strength Index (GSI), as the name indicates, was not developed for a support classification (Hoek and Brown 1997; Hoek et al. 1995) but to characterize the rock mass to obtain rock mass strength properties, such that the support can be designed by the use of numerical models, i.e., to assess the rock mass behaviour and

⁹ The Q-system is based on data from civil engineering tunnels and the RMR-system is largely based on data from room and pillar mining; in both systems on a case data base with relatively limited excavation-induced deformations.

4 >> DEFORMATION-BASED SUPPORT SELECTION FOR STRESS-FRACTURED GROUND

its effect on the support. The GSI-system was also developed and mostly calibrated on civil tunnelling rather than on deep mining projects with dominant mining-driven deformations.

These systems therefore typically do not account for deformations resulting from rock mass bulking.

4.3.1 Limitations of rock mass rating systems for conditions with large mining-induced stress changes

Because of the origin and the underlying data base, the applicability of rock mass rating systems is limited to conditions where the deformations are excavation-induced, i.e., for support of declines, shafts, caverns, etc., that are remote from mining (undercut fronts or cave influences, abutments and active draw areas). They are only directly applicable as long as the advancing face causes the rock mass damage.

Support designs based on these rock mass rating systems may not be valid for conditions where mining-induced stress changes deepen the excavation damage zone, cause stress relaxation, and when mining-induced straining leads to elevated rock mass bulking factors. The impact of strain- and confinement-dependent bulking and stress path-dependent deepening of the depth of failure typically leads to non-conservative support designs.

The RMR system was expanded by Laubscher and Jakubec (2002) to MRMR systems with adjustments for weathering, orientation, blasting, water and mining-induced stress, but did not account for bulking aspects for support design.

As indicated above, the GSI system is intended for rock mass characterization only, i.e., to obtain parameters for numerical modelling. Unfortunately, the GSI is often not applicable for hard rock at depth and continuum models, for which the GSI was developed, are also not applicable (see below).

In summary, rock mass rating systems can be used to classify the ground (e.g., for domaining) but should not be used to select rock support for excavations experiencing significant mining-induced stress-fracturing

and related bulking deformations. The rock mass characterization systems (GSI) should not be used without modification for support modelling when mining-induced stress-fracturing and related deformations are anticipated.

4.3.2 Limitations of analytical/numerical models in conditions with large mining-induced stress changes

Most analytical models are based on conventional failure criteria with peak and residual strength criteria and an elastic-plastic or elastic-brittle plastic post-peak constitutive model. These models implicitly assume that the cohesion and frictional strength components are reduced simultaneously, a behaviour that is rarely applicable to brittle, hard rocks (Hoek and Martin 2014). Furthermore, the adopted deformation models are based on flow rules that are associated with the adopted yield criterion or, if not, depend on an assumed dilation parameter. These models typically are not suitable to simulate the geometric bulking process as the uni-directional bulking, perpendicular to the excavation boundary, is not isotropic (as assumed in most continuum constitutive models). As a consequence, these models tend to underestimate radial straining in the area relevant for support design (i.e., near the excavations) and overestimate the build-up of stabilizing tangential (hoop) stresses.

Attempts have been made by many to circumvent these issues when simulating brittle failure, e.g., by use of brittle Hoek-Brown parameters (Martin et al., 1999) or bi-modal failure envelopes (Diederichs et al. 2010). Some of these have been successful in modelling the extent of damage (the depth of failure) but they are generally inadequate for strain and deformation modelling and thus inadequate for the purpose of support design. The effect of rock reinforcement on rock mass bulking and, visa versa the effect of bulking on support straining cannot be properly simulated by these approaches. As a consequence, the effect of rock mass bulking on support straining has to be estimated separately. As was illustrated by the GRCs in Figure 20, rock mass bulking often adds substantial extra deformation and thus can dominate support straining.

Elastic-brittle plastic models with high post-peak strength loss models have also been used to simulate the extent of failure, but these models often use stress-strain behaviours that are not representative for rock types encountered in deep mining operations (i.e., rocks that require substantial straining before reaching the residual strength (see Kaiser 2016; ISRM lecture). They are also inadequate to assess bulking strains and related rock mass deformations and thus are equally limited for support design in rock experiencing significant mining-induced stress damage. Recent work by Walton and Diederichs (2014 and 2015), while potentially promising to mitigate some of these limitations, still does not capture the impact of reinforcement on the rocks bulking characteristics.

Until models are available to properly simulate brittle failure, related bulking and support behaviour, the anticipated support deformation from unidirectional bulking has to be assessed separately and superimposed on the deformations obtained from continuum models (see Section 4.6).

4.4 RECENT DEVELOPMENTS IN MODELLING FOR DEFORMATION-BASED SUPPORT DESIGN

Because empirical support design approaches and analytical or numerical continuum models are not suitable to simulate brittle failing rock and rock exhibiting geometric bulking¹⁰, Itasca Ltd. is in the process of developing the bonded block model (BBM) approach with improved support elements for discontinuum modelling. This discontinuum-modelling tool, employing a bonded block model (BBM), captures the most essential behavioural elements for a deformation-based support design. The BBM produces very promising results but further developments and validations are required before they can be applied on a routine basis, especially as it pertains to the intense straining of ground support at explicit fractures subject to both shear and extension.

¹⁰ They tend to underestimate the bulking related convergence and strains imposed on support elements.

4 >> DEFORMATION-BASED SUPPORT SELECTION FOR STRESS-FRACTURED GROUND

Figure 22 presents an example output of a tunnel in a BBM subjected to vertical loading and unloading by an advancing undercut. Stiff bolts are modelled for the left wall and debonded bolts for the right tunnel wall. The relaxed stress-fractured zone with related bulking is clearly visible (shown in black) and drastically different bolt responses are evident with bolt failures on the left and distributed bolt yield on the right. This example shows that recent developments are most promising for the purpose of proper support modelling in stress-fractured, bulking ground. Most importantly, it illustrates that large deformations (>0.15 m in this case) impact the bolt response near the walls and this confirms that the support needs to be selected on deformation-based criteria when intended for the control of brittle failure processes.

Until numerical models are developed and calibrated to overcome the various remaining deficiencies of numerical models, semi-empirical means have to be adopted whereby the effect of bulking is assessed independent of the adopted numerical model. These consist of two overall components: determination of anticipated bulking deformation demand and matching of the support system's deformation capacity to the deformation demand.

4.5 'GABION SUPPORT' CONCEPT FOR SUPPORT OF STRESS-FRACTURED GROUND

A gabion (from Latin *cavea* meaning «cage») is a cage filled with rocks for use in civil engineering, road building, military and landscaping applications¹¹. A gabion wall is a retaining structure made of stacked stone-filled gabions tied together with steel mesh (Figure 23a). Internal to each gabion, bulking is controlled by the mesh resisting desired movements of individual rocks; i.e., the gabion reduces the ability of rock fragments to rotate and move relative to each other, thus preventing or at least restraining the bulking process¹².

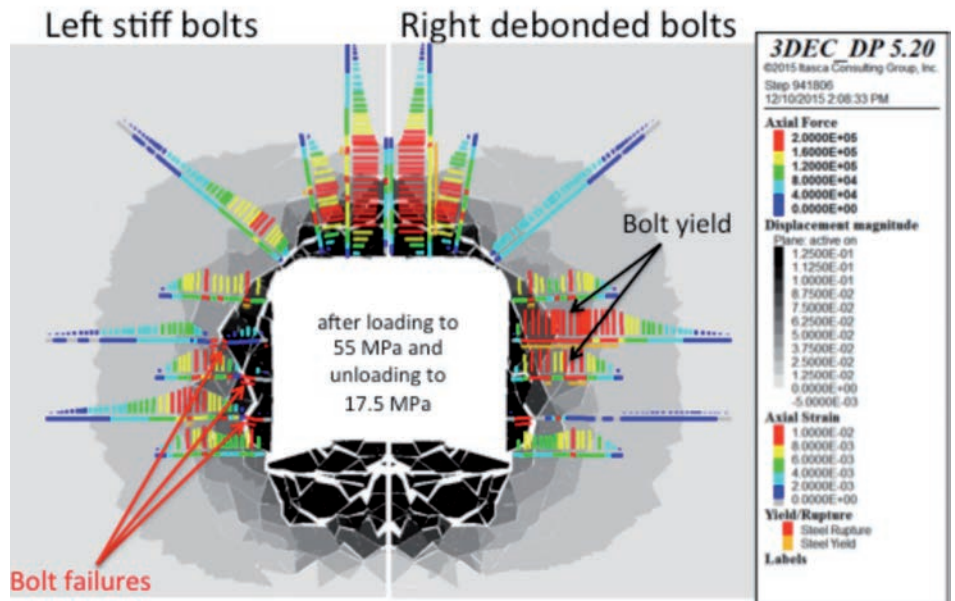


Figure 22 : Example output of a bonded block model after the tunnel was exposed to a loading and unloading cycle: Left side supported by stiff bolts and right side supported by debonded bolts (an internal pressure of 0.1 MPa was applied to mimic the effect of a deformable retention system/surface support) (Courtesy: Itasca Ltd.).

By analogue, the “gabion support” concept for ground control was developed by Kaiser in 2012 to support stress-fractured ground (illustrated by the Voronoi model in Figure 23b). As discussed above, this stress-fractured ground becomes prone to bulking during mining-induced relaxation. By creating stacked gabions of stress-fractured rock (Figure 23c), retained by mesh or shotcrete and tied together with rockbolts or cables, the benefits of the gabion retaining system can be captured for the control of large mining-induced deformations.

Such “support gabions” provide bulking control, superior retention capacity, add confinement to the ground behind (blue lateral arrows), and enhance the tangential load bearing capacity (blue vertical arrows) to reduce roof sag (or floor heave). Furthermore, it retains broken rock (white zone in Figure 23b) during the confinement loss in unloading situations (Figure 21c).

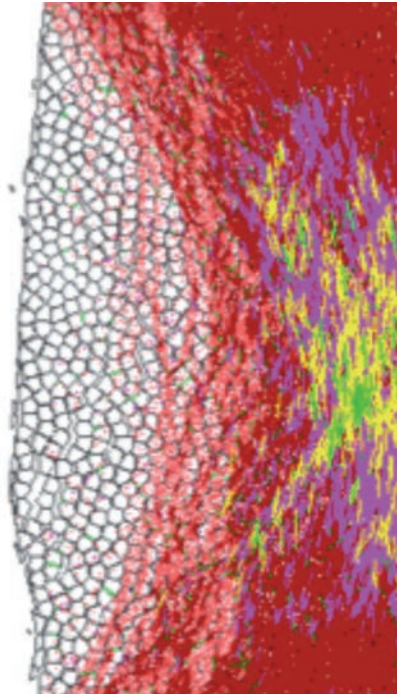
Gabion support offers several advantages over more rigid support structures because they can conform with imposed deformations and can dissipate energy if dynamically loaded. The strength and effectiveness of a gabion support system depends on the strength and size of the retained broken rock, and the ductility and strength of the adopted retention/ reinforcement system. The gabion support concept provides the framework for a fundamental shift to a deformation-based support selection.

¹¹ Leonardo da Vinci first designed a type of gabion, called a Corbeille Leonard («Leonardo basket»), for the foundations of the San Marco Castle in Milan, Italy.

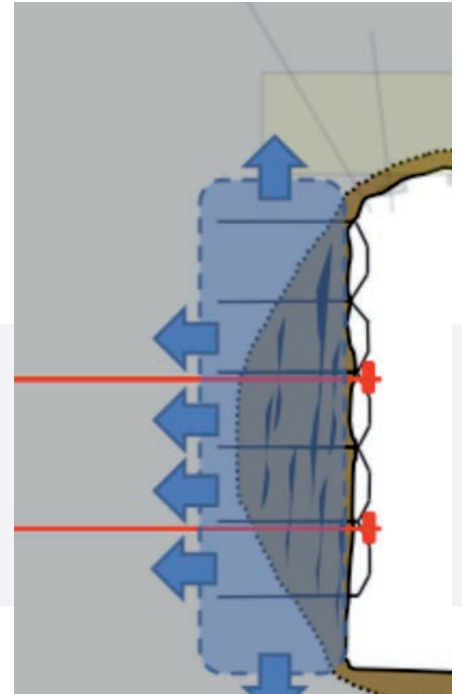
¹² Note: It is the local deformation or strain control by the steel mesh rather than the imposed confining pressure that reduces the bulking. Hence, it is the deformation constraint provided by the retaining system tied to dense bolting rather than the support pressure provided by a shotcrete that affects the bulking in the inner shell, close to the excavation.



(a)



(b)



(c)

Figure 23 : (a) Gabion retaining wall (Photo by Acanfora (CC BY-SA 3.0 via https://commons.wikimedia.org/wiki/File:Gabion_040.jpg); (b) deformed shape of Voronoi pillar model at 1% tangential strain with major principal stress vectors showing hour-glassing mode of failure; and (c) Gabion support analogue for ground control in walls of drifts (Kaiser 2012).

4 >> DEFORMATION-BASED SUPPORT SELECTION FOR STRESS-FRACTURED GROUND

4.6 DEFORMATION-BASED SUPPORT SELECTION

Geotechnical or geomechanics engineering entails three fundamental principles: identification of relevant failure mechanisms; estimation of design demands and support capacities; and determination of an acceptable safety margin (matching demand and capacity).

A systematic design methodology thus includes:

- understanding and recognizing relevant failure mechanisms;
- selecting support components to form a compatible support system based on specific roles and functions;
- selecting an applicable factor of safety concept (in terms of load, deformation and/or energy);
- identifying design demands: load, deformation or energy; and
- selecting the most desirable support component as well as support system capacities (again in terms of load, deformation and energy dissipation).

4.6.1 Relevant failure mechanisms

In brittle failing ground, several distinct mechanisms are causing damage to an excavation and its support:

- ravelling of stress-fractured rock after a transition from a coherent (cohesive) to a broken (frictional) rock mass; causing overbreak, stand-up time or fall of ground issues; and
- sudden or gradual volume expansion or bulking of the fractured rock mass near an excavation due to tangential straining; i.e., strain-controlled bulking of stress-fractured rock.

The significance of the bulking process in support design is often not recognized, even though it is now evident that it accounts for a substantial amount of observed support damage.

Identification of the predominant (gravity-versus stress-driven) damage mechanisms forms a fundamental basis for a support design. Each mechanism is to be

considered separately or in combination when selecting support, as the drivers and the consequences may differ. Here we focus on deformation-driven processes. A sound design of course has to be checked against load (wedge) and energy (bursting) criteria.

4.6.2 Support functions in stress-fractured ground

In general, support serves four functions:

- prevention of falls of ground: maintaining a stable equilibrium (wedge stabilization);
- stabilization of stress-fractured ground: managing a skin of broken rock (retention and volume control);
- convergence control: reducing detrimental (tangential and radial) deformation of the supported ground; and
- confinement of the surrounding rock mass by increasing the radial stress to strengthen the rock further away from the excavation (e.g., by confining the pillar core).

The deformation-based support design approach primarily addresses the latter three functions and means of estimating bulking related deformations and support straining are briefly reviewed in the following sections.

Figure 24 illustrates the consequences of a support system that was not able to provide the latter three functions (stabilize broken rock, control convergence, and provide confinement). The failure of the supported bull nose in Figure 24 can be attributed to one or several of the following factors:

- excessive roof to floor convergence (due to roof settlement and/or floor heave; both causing potentially excessive wall parallel or tangential straining of the wall rock or bullnose);
- high strain sensitivity of the stress-fractured ground causing excessive bulking;
- little deformation restraints in the low confinement zone due to unfavourable geometry (pillar or bull nose); and
- rock mass disintegration due to poor blasting practises or high stress near excavation wall.

The first is the driver, causing rock mass degradation with consequential bulking and support loading. The other three weaken the rock and render it prone to ravelling. If there was no roof to floor convergence, the wall rock and the various support components would not get excessively strained.

In other words, the roof to floor convergence



Figure 24 : Failed bull nose supported with bolts, mesh and shotcrete (Photo courtesy S. Talu).

¹³ Note: such measures need to be installed early enough to prevent the onset of failure propagation processes. The often-quoted inability of these measures to stabilize a situation can frequently be attributed to late remedial actions.

4 >> DEFORMATION-BASED SUPPORT SELECTION FOR STRESS-FRACTURED GROUND

in this case was the source of rock mass disintegration and related bulking with consequential loading or straining of the support in the radial direction. Since it is the wall parallel strain that causes the rock and support damage, the support function that can best prevent this damage is the first of the four functions listed above (roof to floor convergence control). Much effort is often spent on constraining stress-fractured, broken rock rather than on reducing the cause, the roof settlement or floor heave near the excavation walls (or bull nose in this case).

The role of the support in such situations therefore is:

- create a stable roof beam that can be anchored to stable, less deforming ground;
- reinforce the rock in the floor close to or underneath the walls, if at all possible, to prevent or minimize floor heave; and
- install roof to floor convergence reduction measures near the walls (e.g., reinforced shotcrete arches, concrete-filled caissons or vertical steel sets).¹³

In summary, deformation-based support design implies utilization of two very important support functions:

- control of roof to floor convergence to minimize tangential wall straining; and
- support of broken rock in the damage zone near the excavation wall (referred to as “gabion support” concept).

4.6.3 Effective reinforcement of broken rock

In addition to the tangential deformation control the support has to:

- maintain the integrity of the excavation (walls and back), i.e., retain the broken, reinforced ground to stop the driving deformation before it reaches the limit of operationally acceptable radial displacement (i.e., typically on the order of 250 mm per wall (500 mm total closure, i.e. $\leq 10\%$ closure strain in mining); and
- minimize bulking of well-retained rock with ductile rock reinforcement, and provide radial support pressure to confine the surrounding ground

If a rock mass with non-persistent joints and defects (e.g., vein stockworks) is highly stressed, joints and defects shear and open in tension (extension) as illustrated by the Voronoi analogue in Figure 17a, and form small but strong fragments or rock blocks. The corresponding horizontal displacement field, parallel to a potential radial bolt, is stepped as shown by Figure 25 for the Voronoi model. For example, at an applied tangential strain of 0.75% (about 38 mm roof to floor convergence near the wall of a 5 m high tunnel), the overall lateral strain is about 0.6% (causing 11 mm wall deformation in the 2 m deep monitoring zone). However, localized strain peaks ranging from 0.5 to 7% are encountered near stress-damaged block boundaries. These localized strain peaks¹⁴ as well as the overall strain grow with increasing tangential deformation. These overall and localized strains, measured by extensometers, are partially or fully transferred to the rockbolts (depending on the bolt type). For the following discussion, it is conservatively assumed that all of the rock strain is transferred to the bolts. In reality, grout deformation and shear at the interfaces between rock and grout and bolt will reduce the actual load transfer.

Ductile steel exhibits a strain-hardening behaviour as illustrated by Figure 26: yield is initiated at 0.2% strain with an initial yield strength plateau (at 450 MPa in this example). The strength then increases during the hardening phase by about 35% until the maximum tensile strength (610 MPa) is reached between 10 and 15% strain and failure occurs in tension at about 400 MPa after a rapid strength loss during necking. Bolts made of such ductile steel can therefore safely tolerate 15 to 20% pure axial strain¹⁵.

Therefore, a bolt made of ductile steel would survive the strain pattern shown in Figure 25¹⁶. It would definitely yield but not reach its full capacity under the overall strain of 0.6%. Furthermore, even if perfectly bonded to the surrounding rock, it would just approach its maximum tensile capacity (at 7% local strain peaks). It would still have about 11% strain reserve before necking starts and about 13 to 18% strain reserve before failure. When

combined with shear at the strain localization points, the bolt might fail at a lower axial strain limit.

This example illustrates that an effective support system for stress-fractured ground requires ductility provided by ductile steel or by high yield capacity (e.g., as could be provided by debonded cables or yielding bolts).

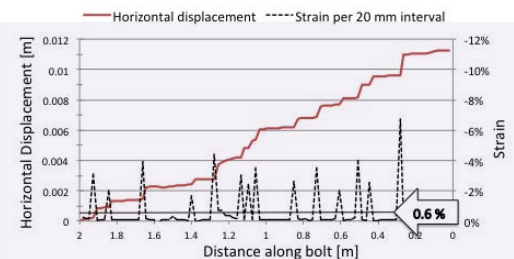


Figure 25 : Schematic illustrations of a displacement pattern along a bolt (red line) and a local strain field in the fractured ground (dashed line for an assumed yield length of 20 mm).

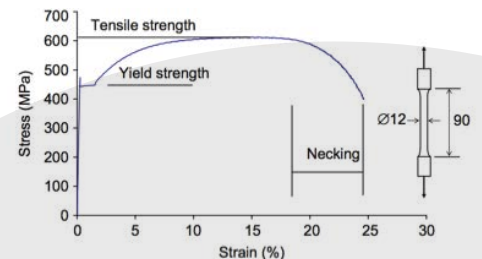


Figure 26 : Typical stress strain-curve of ductile steel with initial yield at 0.2% strain, reaching tensile strength at 10 to 20% strain, and ultimate failure after necking at about 25% strain.

¹⁴ The local strain was calculated for a 20 mm base length, later called “yield length”. A bolt would only experience such strains if the bolt was perfectly clamped by the rock on either side of the 20 mm base length. The localized strain would be half if the displacement step were distributed over twice the base length (e.g., 40 mm due to ground shear failure).

¹⁵ When grouted, the initial stiffness of a bolt is lower and the ultimate failure strain is slightly larger than that of the steel alone. In pure shear, the steel provides a doweling resistance that is typically assumed to be about two thirds of the tensile capacity. Shear also reduces the tensile strength.

¹⁶ If a support component were more brittle, e.g., with only a 3% strain limit, it would break at 7 locations (at intervals of 0.1 to 0.4 m spacing in this case). Hence, rock bolts with at least 7% strain capacity would be required to survive the 0.75% axial tangential strains imposed for the example provided in Figure 25.

4 >> DEFORMATION-BASED SUPPORT SELECTION FOR STRESS-FRACTURED GROUND

Implications for support model parameter selection

When modelling rock bolts in discontinuum models, such as Voronoi models, it is important to match the bolt's stress-strain characteristics well. Often adopted brittleness parameters with low residual bolt strength after yield initiation in elastic, brittle plastic bolt models lead to unreasonably conservative results, as the bolts will fail (drop to residual) at small strains (typically $\ll 1\%$ strain). It is thus necessary to set the residual strength in elastic, brittle plastic bolt models equal to the peak strength and to check whether the failure strain has been reached (not displayed in codes like RS2™).

4.6.4 Estimation of bulking deformation for deformation-based support selection

The deformation-based support selection approach basically consists of comparing the estimated deformation demand with the deformation capacity of each support component in a support system of compatible support components. For this purpose, it is necessary to first establish the deformation demand in the form of a deformation profile (DP) in the zone to be supported and then to compare this deformation profile with the support components' deformation capacity.

Since continuum models cannot account for the unidirectional, geometric bulking of brittle failing rock (see Section 3.4), a semi-empirical approach was developed whereby the bulking deformation is superimposed on the modelled elasto-plastic deformations obtained from continuum models (e.g., continuum displacement profile DP_{Cont} in Figure 27). For this purpose, bulking charts originally introduced based on measurements in South Africa by Ortlepp in Kaiser et al. (1996) have been supplemented and refined by numerical modelling to arrive at the recommended geometric bulking factor BF, presented in the chart of Figure 17d, as a function of the radial confining pressure. This radial confinement can be obtained from numerical continuum models

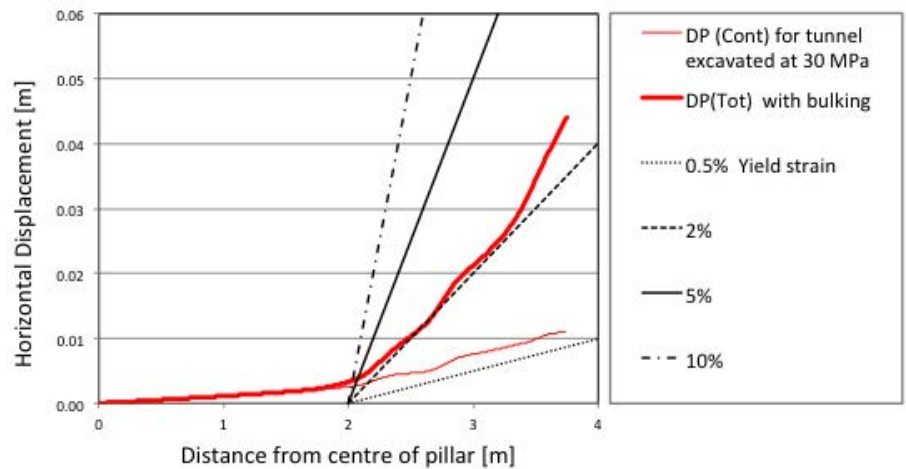


Figure 27 : Schematic example of displacement profiles: light red line from elastic, plastic continuum model and heavy red line without bulking deformation superimposed (simulated extensometer installed in tunnel wall of 7.5 m wide pillar (H:W = 1:1.5); centre at zero); four bolt strain limits are shown for 0.5, 2, 5 and 10% by black lines.

and the bulking strain can be calculated incrementally to obtain the bulking displacement profile $DP_{Bulking}$ (not shown). The total deformation profile DP_{Tot} is then obtained by adding the DP_{Cont} and $DP_{Bulking}$ as shown in Figure 27.

This approach is conceptually illustrated by Figure 27, showing the deformation profiles obtained from the numerical model (DP_{Cont}) and the total deformation profile (DP_{Tot}) after superposition of bulking deformations. Also shown are four potential bolt deformation profiles (BDP), i.e., for bolts that can sustain 2, 5, 10 and 20% yield strain. By comparing the slope of the bolt's deformation profile with that of the rock, it can be seen that about 2% yield will be encountered between 2 and 3 m (5% between 3 m and the tunnel wall). In other words, a support component must have at least 5% yield capacity near the excavation wall¹⁷. A comparison of the bolt's deformation profile with the numerical model (fine line of DP_{Cont}) shows that a bolt with about 0.5% yield capacity would seemingly be adequate but this is not the case because of the bulking deformation resulting in the DP_{Tot} .

The deformation-based support selection approach therefore consists of establishing

the deformation demand (the DP of the rock mass) to assist in selecting support components (bolts or cables) with sufficient deformation or yield capacity (by comparison with the bolts deformation profile).

One complicating factor in this approach is that certain rock reinforcements may not have sufficient yield capacity to survive the imposed deformation demand but still play a positive role by reducing the deformation demand, i.e., by changing the bulking factor and thus the deformation profile of the rock mass. Hence, it is necessary to first determine how the rock reinforcement affects the bulking and then to assess the support's deformation capacity with the appropriate bulking factors for reinforced ground. In practice, this typically leads to a need to install support systems with two types of support components, one to reinforce the rock mass for bulking control and the other to provide sufficient yield capacity. An ideal support component may provide both functions but often it is more efficient to stage support and select supplemental support components, such as cable bolts, to survive large deformations (or to provide a desired safety margin).

¹⁷ If localized deformations are encountered at block boundaries (see Figure 25) more than 5% yield capacity is required.

4 >> DEFORMATION-BASED SUPPORT SELECTION FOR STRESS-FRACTURED GROUND

4.6.5 SUPPORT SELECTION IN STRAINBURST-PRONE GROUND

Strainbursts are sudden, violent excavation failures that may be triggered by a seismic event but are primarily the result of the tangential stress near an excavation exceeding the capacity of the unconfined or lightly confined rock mass due to excavation advance or near-by mining. Damage to the excavations is primarily caused by the sudden creation of a zone of stress-fractured rock, i.e., by the transition to a depth of failure $d/a > 0$. If not supported, this may lead to rock ejection. However, if well supported with an effective support system, all of the released energy is consumed by fracture energy, heat, friction and the deformation of the reinforced rock mass (the “gabion”). In other words, there is no rock ejection and the ejection velocity is zero. Hence, an effective support system has to survive the deformation resulting from the sudden creation of a depth of failure and the related bulking.

Support selection for tunnels in strain-burst prone ground fundamentally consists of assessing the excavation deformation potential by estimating the total post-fracturing deformation profile (as discussed above) and then matching the supports deformation capacity with the suddenly imposed deformation demand. Since all energy will be consumed during the deformation of the reinforced rock mass, there is no remnant energy to be dissipated and the safety margin of a support system in burst-prone ground is obtained by selecting a deformation capacity that exceeds the deformation demand. Kaiser (2014) presents the details of deformation-based support selection for tunnels in strain-burst prone ground. For conditions with dynamic loading by a remote seismic event, energy-based support design principles, as described in Kaiser et al. (1996), are applicable.

From a support design perspective, it follows that strainburst damage can be prevented or most effectively controlled by a support system consisting of robust retention

elements in combination with stiff rock mass reinforcements (minimising bulking) and with yielding bolts that satisfy deformation rather than an energy demand criteria; in other words, by a support system following the “gabion support” concept.

5 >> CONCLUSION AND IMPLICATION FOR CONSTRUCTABILITY

For the economic and safe construction of deep tunnels, a contractor has to be presented with efficient and effective ground control measures, i.e., support classes that can be rapidly installed and are effective in managing stress-fractured ground within complex geological environments and high levels of uncertainties. For this purpose, it is necessary to properly anticipate the actual rock mass behaviour and then provide flexible but reliable means for ground control, i.e., for the support of a shell of heavily stress-damaged ground such that a tunnelling project can proceed without unnecessary delays. Robust engineering in highly stressed, brittle failing rock therefore means to design for rock mass degradation and ensure that all construction tools are working well and are effective.

Guidance is provided for the quantification of anticipated rock mass behaviours and for the selection of design inputs to arrive at safe and efficient ground control measures in stress-fractured ground; ground that is prone to ravelling and large deformations due to rock mass bulking.

The primary conclusions highlight the need for improvements in better anticipating the rock mass behaviour at the tender stage and the need to design ground control measures from a perspective of deformation compatibility as well as practicality rather than theoretical analysis.

Stability assessment

With respect to excavation stability, it is necessary to anticipate brittle failure processes early in the design process such that relevant information can be collected to properly describe the implications of shallow rock mass damage and bulking of stress-fractured ground (e.g., reduction of stand-up time). Today, quantitative means for rock mass characterization are available to provide reliable inputs for simulations of the anticipated extent of failure. Whereas these models can provide guidance for stability assessments, they do neither provide stand-up times in stress-fractured ground nor bulking deformations for support design. Nevertheless, once the failure mode is quantified, constructive measures can

be prescribed for the selection of efficient construction techniques and procedures. For this purpose, it is of utmost importance that the findings of such stability assessments are properly described in tender documents.

Support selection

With respect to ground control, conventional support design approaches using standard rock mass rating systems are severely limited in conditions where stress-driven failure processes dominate. They do not provide effective support systems in stress-fractured ground because they do not account for mining-induced stresses, stress changes, stress-fracturing and related deformations. For tunnelling and mining at depth, it is necessary to select support systems that are effective in controlling the bulking of broken rock and able to yield when strained by deformations imposed by the stress-fractured ground. This can be achieved by following the deformation-based approach described in this article.

In stress-fractured ground, the safety margin should be established based on a comparison of deformation demands and the support's deformation capacity. Since standard numerical models cannot estimate deformations from uni-directional rock mass bulking, it is necessary to separately estimate the deformation demand if bulking is anticipated. The "gabion support" concept was introduced to describe means to stabilize broken rock and to illustrate why deformation-based support selection principles are most suitable for conditions with stress-fractured ground. The purpose of a "gabion support system" is to assist the broken rock mass to become self-supporting, i.e., to provide radial and tangential resistance while deforming and dissipating released energy during the rock mass failure process.

Because numerical models cannot account for unidirectional bulking, semi-empirical means have to be adopted to estimate the anticipated deformations following the deformation-based design approach presented in this article. This includes use of depth of failure charts combined with bulking charts. Further research and field

monitoring will be required to verify the range of applicability of the recommended input parameters.

Constructability

With respect to constructability, it is concluded that conditions of brittle failure must be anticipated early and thus well described in a quantitative manner in tender documents. This should include design inputs relevant for estimating stress-fracturing, for anticipating the extent of rock mass degradation and its impact on stand-up time. Most importantly, flexible and effective support systems (classes) must be provided to manage rapidly changing ground conditions and prevent related delays. From a construction perspective, shaping of excavations to remove stress-damaged rock that is anticipated to bulk often provides a cost-effective means of ground control in situations where the depth of failure is limited. However, scaling is often counterproductive as it causes unnecessary overbreak. Since profile control assists in placing support and in rendering it effective, support systems ensuring immediate contact with the stress-damaged rock are most beneficial for rapid construction.

6 >> ACKNOWLEDGEMENTS

The following individuals have made specific contributions over the years through discussions on various aspects of rock support design: F. Amann (ETHZ), R. Bewick while at RTC-UMC (CEMI), M. Pierce (Itasca), S. Yong (MIRARCO), and from Rio Tinto: A. Moss, A. van As, G. van Hout, S. Talu and R. Hudson (while at Resolution Copper Mine). The efforts of these individuals and the financial support of these companies is thankfully acknowledged.

The work presented here was also financially supported by NSERC (Canada's Natural Sciences and Engineering Research Council) and ORF (Ontario's Research Fund) supporting the SUMIT program (Smart Underground Monitoring and Integrated Technologies for deep mining).

7 >> REFERENCES

1. Barton, N.R., 2013. Shear strength criteria for rock, rock joints, rockfill and rock masses: Problems and some solutions. *Journal of Rock Mechanics and Geotechnical Engineering*, 5: 249-261.
2. Barton, N.R., 2000. *TBM Tunnelling in Jointed and Faulted Rock*. Taylor & Francis or CRC Press, 184 p.
3. Barton, N.R.; Lien, R., Lunde, J., 1974. Engineering classification of rock masses for the design of tunnel support. *Rock Mechanics and Rock Engineering*, 6(4): 189-236.
4. Bieniawski, Z. T. , 1989. *Engineering rock mass classification*. New York, J Wiley.
5. Bieniawski, Z. T., 1984. *Rock Mechanics Design in Mining and Tunnelling*. A.A. Balkema, Rotterdam, 272 p.
6. Bieniawski, Z. T., 1976. Rock mass classification in rock engineering. *Symposium on Exploration for Rock Engineering, Johannesburg*, 97-106.
7. Cai, M., P.K. Kaiser, Y. Tasaka, and M. Minami, 2006. Determination of residual strength parameters of jointed rock masses using GSI system. *International Journal of Rock Mechanics and Mining Sciences*, 44(2): 247-265.
8. Cai, M., P.K. Kaiser, H. Uno, Y., Tasaka, M. Minami and Y. Hibino, 2004. Estimation of rock mass strength and deformation modulus using GSI system – a quantitative approach. *International Journal of Rock Mechanics and Mining Sciences*, 41(1): 3-19.
9. Diederichs, M.S., T. Carter and C.D. Martin, 2010. Practical Rock Spall Prediction in Tunnel. *Proc. of World Tunnelling Congress, Vancouver*, 8 p.
10. Diederichs, M.S., J.L. Carvalho. and T.G. Carter, 2007. A modified approach for prediction of strength and post yield behaviour for high GSI rock masses in strong, brittle ground. *1st Canada-U.S. Rock Mech. Symp.*, 249-257.
11. Diederichs, M.S., P.K. Kaiser and K.E. Eberhardt, 2004. Damage initiation and propagation in hard rock and influence of tunnelling induced stress rotation. *International Journal of Rock Mechanics and Mining Sciences*, 41: 785-812.
12. Diederichs, M.S., 2003. Rock fracture and collapse under low confinement conditions. *Rock Mechanics Rock Engineering*, 36(5): 339-381.
13. Garza-Cruz, T.V., M. Pierce and P.K. Kaiser, 2015. Use of 3DEC to study spalling and deformation associated with tunnelling at depth. *DeepMining'14, ACG* (eds. Hudyma and Potvin), 13 p.
14. Herget, G., 1988. *Stress in Rock*. A.A. Balkema, Rotterdam, 179 p.
15. Hoek (2015). Lecture on "The Art of Tunnelling". www.rocscience.com/learning/hoek-s-corner/lecture-series.
16. Hoek, E. and C.D. Martin, 2014. Fracture initiation and propagation in intact rock – A review. *Journal of Rock Mechanics and Geotechnical Engineering*, 6(4): 287-300.
17. Hoek, E., 2007. *Practical rock engineering*, 2nd ed. Rocscience Inc.
18. Hoek E., 1999. Putting numbers to geology – an engineer's viewpoint. The Second Glossop Lecture – presented to the Geological Society, *Quarterly Journal of Engineering Geology*, 32(1): 1 – 19.
19. E. Hoek and E.T. Brown 1997. Practical estimates of rock mass strength. *International Journal of Rock Mechanics and Mining Sciences*, 34(8): 1165-1186.
20. Hoek, E., P.K. Kaiser and W.F. Bawden, 1995. *Rock Support for Underground Excavations in Hard Rock*. A.A. Balkema, Rotterdam, 215 p.
21. Hoek, E. and E. T. Brown, 1988. The Hoek-Brown failure criterion - a 1988 update. In *Rock Engineering for Underground Excavations, Proc. 15th Canadian Rock Mech. Symp.* 31-38. Toronto,
22. Hoek, E. (1968). *Brittle Failure of Rock*. In *Rock Mechanics and Engineering Practice*, John Wiley & Sons Ltd. London, 99-124.

7 >> REFERENCES

23. Hutchinson, D.J. and M.S. Diederichs, 1996. Cablebolting in Underground Hard Rock Mines, Bitech Publishers Ltd., Richmond, BC, Canada, 406 p.
24. Kaiser, P. K., 2016. SRM lecture on "Challenges in rock mass strength determination for the design of underground excavations". Web-cast March 15, 2016; www.isrm.net/gca/?id=1104
25. Kaiser, P.K., S.M Maloney and S. Yong, 2016. Role of large scale heterogeneities on in-situ stress and induced stress fields. ARMA 16-571 (in press).
26. Kaiser P.K., 2014. Deformation-based support selection for tunnels in strain-burstprone ground. DeepMining'14, ACG (eds. Hudyma and Potvin), 227-240.
27. Kim B-H., P.K. Kaiser, 2012. Approach to characterize rock mass strength considering joint persistence. 7th Asian Rock Mechanics Symp., 15-19 October, Seoul, South Korea, CD, 8p.
28. Kaiser, P.K. and B-H. Kim, 2008a. Rock mechanics challenges in underground construction and mining. 1st Southern Hemisphere International Rock Mechanics Symposium, Perth, Australia, 1:23-38. Hemisphere International Rock Mechanics Symposium, Perth, Australia, 1:23-38.
29. Kaiser P.K. and B-H. Kim, 2008b. Rock mechanics advances of underground construction and mining. Korea Rock Mechancs Symposium, Seoul, 1-16.
30. Kaiser, P. K., 2007. Rock mechanics challenges and opportunities in underground construction and mining. 1st Canada-U.S. Rock Mechanics Symposium, 47 p.
31. Kaiser, P. K., 2006. Rock mechanics consideration for construction of deep tunnel in brittle ground. Asia Rock Mechanics Symposium, Singapore, 12 p.
32. Kaiser, P.K., 2005. Tunnel stability in highly stressed, brittle ground - Rock mechanics considerations for Alpine tunnelling. Geologie und Geotechnik der Basistunnels, GEAT'05 Symposium'06, Zürich, Switzerland, 183-201.
33. Kaiser, P.K., Diederichs, M.S., Martin, C.D., Sharp, J. and Steiner, W., 2000. Underground works in hard rock tunnelling and mining. GeoEng2000, Technomic Publ. Co., 841-926.
34. Kaiser, P.K., D.R. McCreath and D.D. Tannant, 1996. Canadian Rockburst Support Handbook, Mining Research Directorate, Sudbury, Canada, 314 p.; also Drift support in burst-prone ground. CIM Bulletin, 89(998): 131-138.
35. Laubscher D.H., 1990. A Geomechanics Classification system for the rating of rock mass in mine design. Journal of the S. Afr. Inst. Min. Metall., 90(10): 257-273.
36. Laubscher D.H. and J. Jakubec, 2001. The MRMR rock mass classification for jointed rock masses. In: Underground Mining Methods, Engineering Fundamentals and International Case Studies (ed. W.A. Hustrulid & R.L. Bullock), Ch.57: 475-481.
37. Martin C.D., P.K. Kaiser, R. Christiansson, 2003. Stress, instability and design of underground excavations. International Journal of Rock Mechanics and Mining Sciences, 40(7-8): 1027-1047.
38. Martin, C.D., P.K. Kaiser and D.R. McCreath, 1999. Hoek-Brown parameters for predicting the depth of brittle failure around tunnels. Canadian Geotechnical Journal, 36(1): 136-151.
39. Ortlepp, W.D., 1997. Rock Fracture and Rockbursts: an illustrative study. Monograph series M9. South African Inst. Min. Metall. 220 p.
40. Rabcewicz L.V., 1969. Stability of tunnels under rock load: Part 1. Water and Power, 21(6): 225-229.
41. Rojat F., V. Labiouse, P.K. Kaiser, F. Descoeurdes, 2008. Brittle rock failure in the Steg lateral adit of the Lötshberg base tunnel. Rock Mechanics and Rock Engineering, 42(2): 341-359.
42. Sheorey, P. R., 1994. A theory for in situ stresses in isotropic and transversely isotropic rock. International Journal of Rock Mechanics and Mining Sciences, 31(1): 23-34.
43. Steiner W., P.K. Kaiser, G. Spaun, 2011. Role of brittle fracture on swelling behaviour: evidence from tunnelling case studies; Sprödbbruch in wenig festem Fels als Auslöser von Quellvorgängen: Erkenntnisse aus Fallstudien. Geomechanics and Tunnelling, 4(2):583-596.

7 >> REFERENCES

44. Steiner W., P.K. Kaiser, G. Spaun, 2010. Role of brittle fracture on swelling behaviour of weak rock tunnels: Hypothesis and qualitative evidence; Sprödbbruch in wenig festem Fels als Auslöser von Quellvorgängen: Beobachtungen und Analysen. *Geomechanics and Tunnelling*, 3(5): 141-156.
45. Spottiswoode, S.M., L.M. Linzer and S. Majiet, 2008. Energy and stiffness of mine models and seismicity. 1st Southern Hemisphere International Rock Mechanics Symposium, Perth, Australia, 1: 693-707.
46. Walton, G. and M.S. Diederichs, 2014, Dilation and post-peak behaviour inputs for practical engineering analysis. *Geotechnical & Geological Engineering*, 33:1: 15-34.
47. Walton, G. and M.S. Diederichs, 2015. A mine shaft case study on the accurate prediction of yield and displacements in stressed ground using lab-derived material properties. *Tunnelling and Underground Space Technology*, 49: 98-113.
48. Wickham, G.E., Tiedemann, H.R. and Skinner, E.H., 1972. Support determination based on geologic predictions. *Proc. North American Rapid Excavation and Tunnelling Conf.*, Chicago, (eds K.S. Lane and L.A. Garfield), New York, SME, 43-64.

